

HEAT TRANSPORT BY LARGE-SCALE ATMOSPHERIC
WAVES DURING OCTOBER 1959-MARCH 1960

by

Calvin E. Anderson

A thesis submitted to the Faculty of Graduate
Studies and Research in partial fulfilment of the
requirements for the degree of Master of Science.

Department of Meteorology
McGill University,
Montreal.

August 1963.


Table of Contents

	Page
Acknowledgments	iii
List of figures	iv
Abstract	vii
1. Introduction	1
1.1 Data	3
1.2 Method	6
2. Problem	8
2.1 Spectrum of Heat Transport	10
2.2 Total Northward Heat Transport	21
2.3 Mean Temperature Changes and Related Atmospheric Phenomena	35
2.4 Divergence of Heat Transport and Mean Temperature Changes	39
2.5 Stratospheric Vertical Motions	49
3. Conclusions	57
References	60

Acknowledgments

The author conducted this research while on temporary assignment to McGill University, Meteorology Department, from the U.S. Weather Bureau for graduate schooling. This research was done under the direction of Professor B.W. Boville who proposed the project. The author is especially grateful to Professor Boville for his guidance and discussions that made this project possible. The author appreciated the generous help and cooperation received in this study from members of the Arctic Meteorology Research Group at McGill University; the staff at the Central Analysis Office, Montreal Airport, Meteorological Branch, Department of Transport, Canada, and staff at the Stratospheric Meteorology Research Project, U.S. Weather Bureau, Washington, D.C.

List of Figures

Fig.	Page
<p>1. Average northward heat transport (10^{11} joules sec⁻¹ mb⁻¹) at 500 mb, 100 mb and 25 mb as a function of wave number for the period October 5, 1959 through March 28, 1960. Transports were averaged over latitudes 40N to 80N. Dashed line is 25-mb average transport from Boville (1961) for previous six month period of 1958-59.</p>	11
<p>2. Graph of monthly heat transport (10^{11} joules sec⁻¹ mb⁻¹) by wave one for 500 mb, 100 mb and 25 mb. Dashed curve for 25 mb from Boville (1961).</p>	17
<p>3. Graph of monthly heat transport (10^{11} joules sec⁻¹ mb⁻¹) by wave two for 500 mb, 100 mb and 25 mb. Dashed curve for 25 mb from Boville (1961).</p>	18
<p>4. Graphs of monthly heat transport (10^{11} joules sec⁻¹ mb⁻¹) by wave three and four each for 500 mb, 100 mb and 25 mb. Dashed curves for 25 mb from Boville (1961).</p>	19
<p>5. Total heat transport by waves one through twelve for the period October 5, 1959 through March 28, 1960. Northward transport is positive, southward transport is negative (stippled). Charts (a), 500 mb, at intervals 2×10^{12}; (b), 100 mb, at intervals 3×10^{12}; (c) 25 mb, at intervals 4×10^{12} joules sec⁻¹ mb⁻¹. Blocks, ; in fig. 5(c) enclose sign of correlation between the 25-mb and the 500-mb levels shown in fig. 5(d).</p>	23

- 5(d). Explanation same as 500-mb chart in fig. 5(a), except transport values are for waves one, two and three only. 25
- 5(e). Total heat transport by waves one through nine for period October 5, 1958 through March 29, 1959 at 25 mb. Northward transport is positive, southward transport is negative. (10^{12} joules sec^{-1} mb^{-1}). From Boville (1961). 27
6. Total heat transports at all levels for the period 12-16 January 1959. In each cell the total transport is plotted in the vertical and latitude decreases to the right. Heavy curves are a pressure-day locus of minimum transport. A, B and C are maxima which progress northward with time. From Hill (1963). 33
7. Mean temperature ($^{\circ}\text{C}$) profiles at 500 mb, 100 mb and 25 mb from selected latitudes 35N, fig. 7(a), and 65N, fig. 7(b), for period October 5, 1959 through March 28, 1960. Temperature profiles at 500 mb are inverted for comparison with stratosphere. Temperature values were obtained from means computed in the Fourier series. 36

Fig.		Page
8.	Mean temperature ($^{\circ}\text{C}$) charts for period October 5, 1959 through March 28, 1960. Charts (a), (b) and (c) are the 500-mb, 100-mb and 25-mb levels respectively.	40
9.	Calculated temperature change charts for $^{\circ}\text{C}$ per day computed from time derivatives of the divergence of total heat transport for period October 5, 1959 through March 28, 1960. Charts (a), (b) and (c) are the 500-mb, 100-mb and 25-mb levels respectively, for waves one through twelve. Areas of convergence are positive and divergence are negative (stippled).	45
9(d).	Explanation same as fig. 9(a) except computations are from 500-mb heat transport chart in fig. 5(d).	46
10.	Heat transport "budget" charts ($^{\circ}\text{C}$ per day) for period October 5, 1959 through March 28, 1960. Chart (d) is the 500-mb level for waves one, two and three. Charts (b) and (c) are the 100-mb and 25-mb levels respectively, for waves one through twelve. (stippled area negative).	48
11.	Schematic cross-section of temperature and streamlines of vertical motion for January 8, 1960. Temperatures, $^{\circ}\text{C}$, on left (dashed lines) and vertical motion, cm sec^{-1} , on right (solid lines represent meridional flow) of each point.	52

Abstract

A spectral analysis of northward heat transport in the northern hemisphere was performed by the Fourier analysis method. This method was applied at 500 mb, 100 mb and 25 mb for five-day intervals from October 5, 1959 through March 28, 1960. A comparison of stratospheric warmings of this period with those of the previous year studied by Boville (1961), revealed that the heat transport could be accomplished mainly by wave numbers one and/or two. From 500-mb, 100-mb and 25-mb time-sections of northward heat transport, divergences were determined to calculate the local temperature time derivatives. These derivatives were in turn compared with the actual time-sections of mean temperature. This comparison showed that, due to strong convergence of northward heat transport, the winter stratosphere at high latitudes had a net ascending motion.

1. Introduction

The general circulation of the atmosphere is maintained by energy exchange processes which provide energy to compensate frictional losses. To balance this dissipation of energy, three main energy exchange processes have been defined (Lorenz 1955 and others) which essentially account for the observed prevailing currents that constitute the general circulation. Heretofore, studies have emphasized only two of these processes, the conversion between eddy available potential energy and eddy kinetic energy or between eddy kinetic energy and zonal kinetic energy. A measure of the first mentioned process is proportional to the covariance of temperature and vertical velocity, the second is proportional to the transfer of angular momentum.

This study is concerned primarily with the third energy exchange process. This process, the conversion between zonal available potential energy and eddy available potential energy, is more directly related to the differential radiational heating of the atmosphere from the equator to the pole. To minimize extreme temperature differences that would thus develop, the available potential energy is transferred from zonal to eddy flow and is referred to as heat transport. The main transfer is accomplished by horizontal eddies, which are most effective between latitudes 30N and 80N. The actual conversion is proportional to the product of heat transport and the mean poleward temperature gradient. This study is focused mainly on a detailed study of northward heat transport and related aspects. No attempt is made to arrive at energy exchange values.

Relatively few spectral studies of heat transport are found in scientific literature. The required hemispheric specification involves processing vast quantities of data; hence only a few selected levels, at short intervals of time constitute most studies (MINTZ 1955), (Benton and Kahn 1958) and (Van Mieghem, Defriese and Van Isacker 1959). Most of the existing articles present somewhat isolated findings and are therefore difficult to compare, hence the results fail to establish a continuous record. Only recently have meteorological hemispheric charts become available to facilitate heat transport studies in the stratosphere (Boville 1961 and Murakami 1962). Thus to obtain a more comprehensive description of the heat transport spectrum, the 500-mb, 100-mb and 25-mb height and temperature fields were studied at 5-day intervals for the six month period of October 5, 1959 through March 28, 1960.

A study of only the stratosphere was originally intended; however in view of our scant knowledge of the upper atmosphere, it seemed reasonable to include a tropospheric level. The 500-mb and 25-mb levels were therefore selected as representative of the troposphere and stratosphere respectively, since these levels vertically separate the mass of the stratum which they represent by nearly equal amounts. The 100-mb level was included to provide some vertical continuity and to represent the lower stratosphere, which is generally true for latitudes north of 40N.

To gain added insight on the dynamics of the atmosphere, the phenomenon of stratospheric warmings was examined by the spectrum of heat

transport. These warmings are particularly interesting in that the stratospheric flow can reverse from a winter polar-night low to nearly typical warm summer polar high pressure circulation within about two weeks. At times, after strong stratospheric warmings, the polar low pressure center never fully regains its normal wintertime intensity. The following chronological listing of recent stratospheric warmings (Boville 1961) indicates the range of time in which these warmings can occur: The 1956-57 and 1957-58 winter warmings began in late January, in the winter of 1958-59 the warming began in early March 1959. This study shows that the 1959-60 warming was delayed until late March 1960. However these warmings may occur as late as the month of May.

1.1 Data

The data were selected from the 500-mb, 100-mb, and 25-mb 0000Z constant pressure hemispheric charts for the interval of five days from October 5, 1959 through March 28, 1960. These charts were obtained from two sources; the 25-mb charts in "An Atlas of Stratospheric Circulation April 1959-May 1960" (McGill University 1962), 100-mb charts analyzed by the McGill University Arctic Meteorology Group (unpublished) and 500-mb charts from the Canadian Department of Transport. Although these charts were hemispherical, the plotting of additional data was necessary for complete coverage extending down to latitude 30N. The source of data for extended regions and late data was the 'Northern Hemisphere Data Tabulations' of the U.S. Weather Bureau.

To complete the set of 500-mb and 100-mb charts the author extended and revised the analyses where necessary and analyzed all of the corresponding temperature fields for the period of the study. It

would have been desirable to perform a differential analysis for all levels, however, this was not feasible. This deficiency was partially remedied by performing vertical consistency checks in regions of added data. This was achieved by checking the position of surface fronts with respect to the vorticity advection at 500 mb and by an estimation of thermal wind changes in relation to the temperature field. In addition, low level charts were consulted on a daily basis whenever the positions of pressure systems and jet streams were questioned.

The maps were drawn on hemispheric $1 : 20 \times 10^6$ polar stereographic charts true at latitude 60N. These charts were analyzed for intervals of 200 ft at 500 mb, 400 ft at 100 mb and also 400 ft at 25 mb (However the 25-mb charts were published for 800 ft intervals). The isotherms were analyzed at 5°C intervals for all levels. All grid point values were recorded and punched to the nearest 100 ft. and 1°C .

In upper air work pressure, P , is an independent variable and geopotential height, Z , is the dependent variable which is computed from the hydrostatic equation of the form

$$Z = \frac{R}{g} \int_P^{P_0} T d \ln P \quad \begin{array}{l} \text{where } R = \text{gas constant} \\ g = \text{gravity} \\ T = \text{temperature} \end{array}$$

This equation is readily solved with values received from radiosonde instruments, the accuracy of which is usually given as pressure, $P \pm 3$ mb, and temperature, $T \pm 0.5^\circ\text{C}$. At any particular level the accuracy of Z depends on the amount of systematic error in P and T . The accuracy is a function of P and its standard error is usually considered to have the following approximate values: 500 mb, 50 ft; 100 mb, 125 ft and

25 mb, 300 ft (Boville 1961). Solar radiation incident of radiosonde instruments also contributes to instrumental error (Teweles and Finger 1960).

Wind reports contain various instrumental errors, such as target hunting, but their main limitations in the stratosphere are due to range and elevation angle. The standard vector errors following Muench (1958) are approximately:

Rawinsonde, approximate vector error (kt).

	Troposphere	Lower and Middle Stratosphere	Upper Stratosphere
Strong winds	1 - 5	5 - 10	10 - 30
Light winds	1 - 5		

Van Mieghem (1960) has pointed out that any spectral analysis is very sensitive to averaging processes since daily values can vary excessively from day to day. Thus a comparison with other studies must be accepted with caution, especially in the case of different time intervals. Hence it was difficult to compare the preliminary phases of this work with the few existing heat transport studies.

For a meaningful study of the stratosphere, current studies suggest that general circulation work should be conducted over a period of more than one year. That is, the interchange of energy between the large scale atmospheric waves result in a different spectrum from year to year. To meet this need the Meteorology Department at McGill University is directing much of its research toward an extensive stratospheric study for the period 1958-61. This study, for the period

1959-60 is in essence a continuation of the long range research program at McGill University and where applicable it is statistically comparable to Boville's (1961) work for the 1958-59 period.

1.2 Method

The meteorological parameters, height and temperature of a constant pressure surface, are treated as a function of longitude, λ . Height and temperature are single valued functions specified for a given latitude, ϕ , and can be represented by the sum of sine and cosine functions. For such a distribution about a closed latitude circle, the treatment of these meteorological parameters by Fourier analysis has been shown applicable by Boville and Kwizak (1959), Godson (1959), Van Mieghem (1960) and others. This method provides a spectral analysis of the atmosphere whereby the contributions of a parameter can be examined by harmonics (or wave numbers).

Thus these parameters are represented by a Fourier series and written

$$f(\lambda) = a_0 + \sum_{m=1,2,3\dots}^{\frac{N-1}{2}} (a_m \cos m\lambda + b_m \sin m\lambda) \quad (1)$$

where N = number of equally spaced data points on a latitude circle

n = wave number, the number, of integral waves around a latitude circle.

Thus $n = \frac{2\pi R}{L}$, where R is the radius of the latitude circle and L

is the wave length, and λ is longitude, expressed in radians. The

maximum number of waves depends on the data points and is given by

$\frac{N-1}{2}$ (the so-called Nyquist frequency).

To evaluate the coefficients, the integrals are converted to summations in the normal manner. Starting at Greenwich meridian, the latitude circles are divided into 10 degree intervals ($\Delta\lambda = \frac{\pi}{18}$) of longitude. Thus

$$\frac{1}{2\pi} \int_0^{2\pi} f(\lambda) d\lambda = \frac{\Delta\lambda}{2\pi} \sum_{N=1}^{36} f(\lambda)_N = \frac{1}{36} \sum_{N=1}^{36} f(\lambda)_N$$

Hence the Fourier coefficients become

$$a_0 = \frac{1}{36} \sum_{N=1}^{36} f(\lambda)_N$$

$$a_m = \frac{1}{18} \sum_{N=1}^{36} f(\lambda)_N \cos m\lambda \quad n = 1, 2, 3 \dots$$

$$b_m = \frac{1}{18} \sum_{N=1}^{36} f(\lambda)_N \sin m\lambda \quad n = 1, 2, 3 \dots$$

Because of the orthogonality of the trigonometric terms, all sets are integrated over the interval $0-2\pi$ to eliminate cross product terms. Thus the series (1) can be written

$$f(\lambda) = a_0 + \sum_{m=1}^{\frac{N-1}{2}} (c_m \cos(m\lambda - \Theta_m)) \quad (2)$$

where

$$c_m = \sqrt{a_m^2 + b_m^2} \quad (c_m \text{ is the amplitude})$$

and

$$\tan \Theta_m = \frac{b_m}{a_m} \quad (\Theta_m \text{ is the phase angle})$$

2. Problem

The northward transport of sensible heat now can be computed from the given fields of temperature, T , and geopotential height, Z . The use of the geostrophic approximation restricts the computation to the horizontal eddy component of the northward transport, i.e., to the covariance \overline{Tv} where v is the northward component of the geostrophic wind. The expression for northward heat transport, H_T , through a vertical strip of one millibar, at pressure P , extending over all longitudes along a given latitude now may be evaluated and is written as

$$H_T = \frac{2\pi R c_p}{g} \overline{Tv} \Delta P$$

where R = radius of latitude circle, c_p = specific heat at constant pressure and g = gravity. To evaluate \overline{Tv} , the temperature is approximated by the Fourier series

$$T = a_0 + \sum_n (a_n \cos n\lambda + b_n \sin n\lambda)$$

and the meridional wind is represented geostrophically by

$$v = \frac{g}{f} \frac{\partial Z}{\partial \lambda} = \frac{g}{fR} \frac{\partial Z}{\partial \lambda}$$

where f = coriolis parameter and x = distance along latitude circle

and the Fourier series of Z is

$$Z = A_0 + \sum_n (A_n \cos n\lambda + B_n \sin n\lambda)$$

Hence

$$\overline{TV} = \frac{g}{2\pi f R} \int_0^{2\pi} \sum_n [(a_n \cos n\lambda + b_n \sin n\lambda)(B_n \cos n\lambda - A_n \sin n\lambda)]$$

and

$$\overline{TV} = \frac{g}{2fR} \sum_n (a_n B_n - A_n b_n) \quad (3)$$

Substituting (3) into (2) results in heat transport for a given wave number and is written

$$H_T = \frac{0.660 \times 10^{10}}{\sin \phi} \sum_n (a_n B_n - b_n A_n) \text{ joules sec}^{-1} \text{ mb}^{-1} \quad (4)$$

Data were extracted from a polar cap grid that extended from latitude 30N to 80N with grid points at every intersection of 5 degrees latitude and 10 degrees longitude. The same grid was used at 500-mb, 100-mb and 25-mb levels for the fields of geopotential height and temperature giving a total of 85,536 pieces of input data. These data were punched on cards and programmed on the I.B.M. 1410 digital computer at McGill University. The program was written by Capt. Charles E. Hill, USAF. The output consisted of the mean, A_0 , total variance, σ^2 , for each latitude; and the Fourier coefficients A_n , B_n , and C_n , plus the phase angle, Θ . Although this study pertains mainly to long waves, wave numbers were computed out to $n = 12$ as a control on the accuracy of the data.

A significance test was not run on these data. But the significance of wave number was not considered crucial, since this study was restricted to long waves. Boville (1961) found, from a Fourier analysis of similarly assembled data for 1958-59, that the wave numbers were significant down to number 8 at 500 mb, number 7 at 100 mb and number 4 at 25 mb (see Godson 1959).

2.1 Spectrum of Heat Transport

At various stages of this study it became evident that, while the integrated heat transport over the globe should be nearly constant from year to year, significant variations in the heat transport spectrum existed with respect to time and height. The similarity in magnitude of yearly total heat transport at stratospheric levels is suggested by the comparison of the two 25-mb curves that appear in fig. 1, where the dashed curve is for the 1958-59 period (Boville 1961) and the solid curve is for the period of this study. The curves of fig. 1 are all in units of 10^{11} joules sec^{-1} mb^{-1} and a function of wave number averaged over the same six month period.

The heat transport values of fig. 1 were constructed from tabulations entered in table 1. The tables 1(a), 1(b) and 1(c) are average monthly northward heat transport values during 1959-60 at 500 mb, 100 mb and 25 mb, respectively, for waves 1 through 9. From computer output, these monthly values in units of 10^{10} joules sec^{-1} mb^{-1} were obtained at intervals of 5 degrees latitude by averaging over the 9 latitude circles from 40N to 80N. Each month was a sample that consisted of six days at 5-day intervals. In table 1(a), the calculations were extended to wave 10.

TOTAL NORTHWARD HEAT TRANSPORT

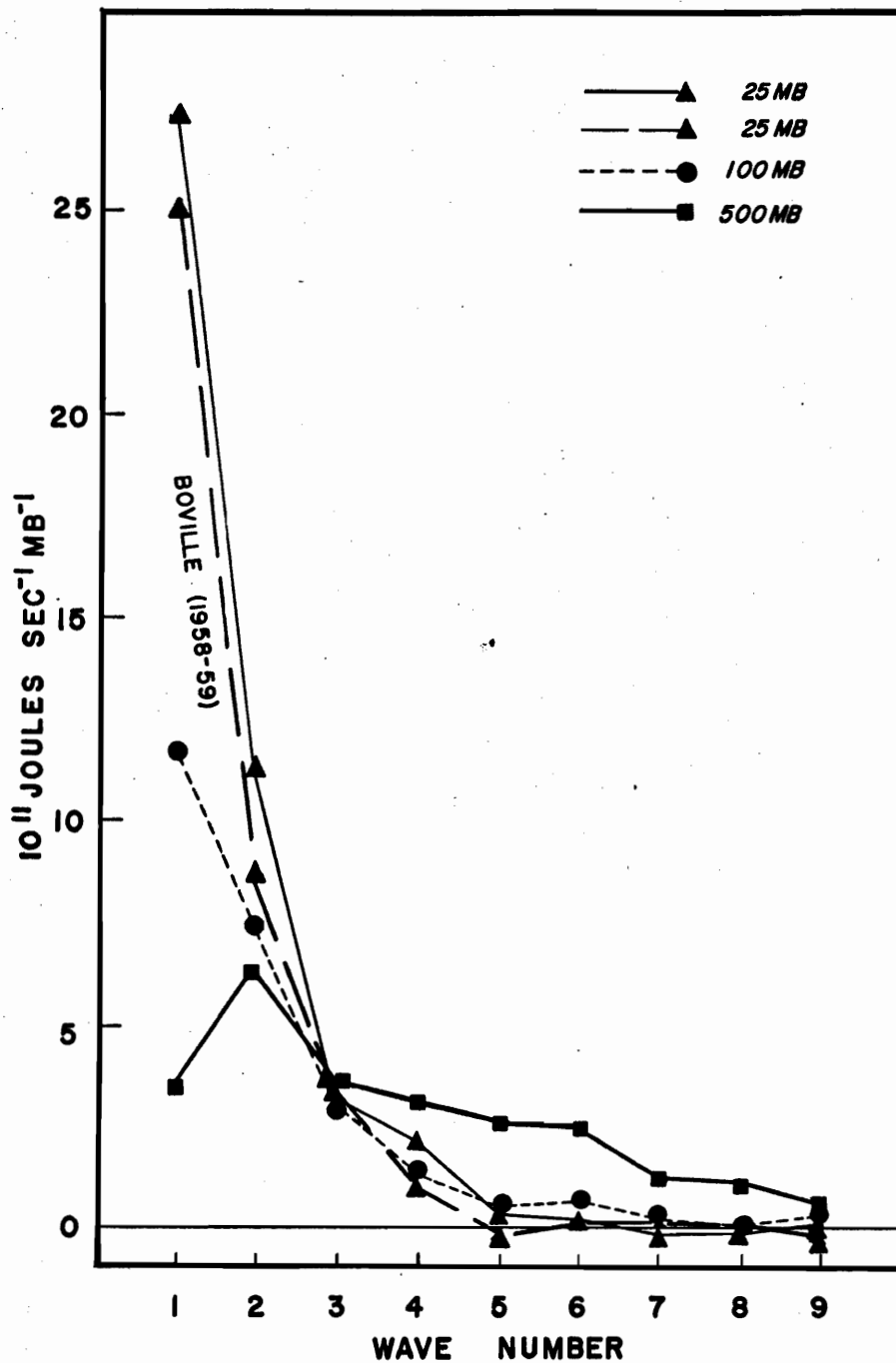


Fig. 1. Average northward heat transport ($10^{11} \text{ joules sec}^{-1} \text{ mb}^{-1}$) at 500 mb, 100 mb and 25 mb as a function of wave number for the period October 5, 1959 through March 28, 1960. Transports were averaged over latitudes 40°N to 80°N . Dashed line is 25 mb average transport from Boville (1961) for previous six month period of 1958-59.

Table 1(a). Average monthly 500-mb northward heat transport
 $(10^{10} \text{ joules sec}^{-1} \text{ mb}^{-1})$ by wave number. Values
 were averaged over latitudes 40N to 80N.

n	1959			1960			Average
	Oct.	Nov.	Dec.	Jan.	Feb.	Mar.	
1	39.1	43.4	50.0	27.1	37.0	2.0	33.1
2	41.5	64.4	70.0	121.5	43.7	51.7	65.5
3	35.2	21.5	10.1	68.4	63.3	27.6	37.7
4	43.3	21.9	40.6	5.5	45.8	27.2	30.7
5	16.4	27.8	33.8	54.1	25.3	6.2	27.3
6	27.1	14.0	33.4	25.5	30.3	28.6	26.5
7	6.0	9.9	9.3	22.5	18.1	13.1	13.1
8	6.0	9.6	7.9	10.4	18.5	12.3	10.8
9	15.7	5.2	6.6	4.7	5.4	7.2	7.5
10	2.5	1.7	2.7	3.0	2.4	4.0	2.7

Table 1(b). Average monthly 100-mb northward heat transport
 $(10^{10} \text{ joules sec}^{-1} \text{ mb}^{-1})$ by wave number. Values
 are averaged over latitudes 40N to 80N.

n	1959			1960			Average
	Oct.	Nov.	Dec.	Jan.	Feb.	Mar.	
1	28.4	114.3	155.5	174.7	189.8	46.8	118.3
2	21.0	96.9	89.3	105.1	39.7	103.0	75.8
3	12.0	34.9	38.3	73.4	26.5	2.8	31.3
4	21.3	9.8	2.8	20.0	5.9	24.6	14.1
5	5.5	-4.0	13.5	0.9	6.7	2.8	4.2
6	3.1	4.0	13.7	15.0	-1.3	1.7	6.0
7	-1.3	2.7	3.3	6.6	-2.1	2.2	1.9
8	-0.6	-0.8	-0.4	4.1	-2.3	2.7	0.5
9	1.0	1.7	0.1	2.9	1.2	2.1	1.5

Table 1(c). Average monthly 25-mb northward heat transport
 $(10^{10} \text{ joules sec}^{-1} \text{ mb}^{-1})$ by wave number. Values
 are averaged over latitudes 40N to 80N.

n	1959			1960			Average
	Oct.	Nov.	Dec.	Jan.	Feb.	Mar.	
1	24.6	165.1	327.7	603.6	363.0	159.9	274.0
2	31.3	169.3	146.5	84.2	111.5	141.7	114.1
3	8.3	59.2	79.9	23.9	26.6	0.5	33.1
4	12.2	37.5	-5.9	70.9	0.9	24.5	23.3
5	1.2	11.3	4.5	1.4	1.3	-3.7	2.7
6	0.9	-1.4	5.6	0.0	1.9	5.1	2.0
7	-0.6	-1.4	1.4	0.1	1.0	-1.0	-0.1
8	-0.1	0.3	0.3	-0.3	-0.9	0.4	-0.0
9	0.2	-0.6	0.8	0.8	-0.4	0.3	0.2

A slight yearly deviation of 25-mb heat transport is noted for each wave number (fig. 1), however these differences are probably comparable to the error inherent in the methods employed. Since a similar study for 1958-59 at 500 mb and 100 mb was not available, this comparison could not be extended to lower levels. However, masked in these six month averages are salient features of monthly heat transport which are of considerable interest.

A comparison of average monthly northward heat transport for 1959-60 with the transport values of 1958-59 (Boville 1961), suggests that stratospheric warmings may be accomplished by several combinations of long waves. Also the ratio of per millibar heat transport values between the stratosphere and troposphere for a given wave number slowly changed throughout the period studied. For the levels studied these per millibar values of long wave transport were either the largest at 25 mb, as expected, or at times were nearly equal to the 500 mb-level. Thus it was found that, in this respect, the mechanism of heat transport may differ annually.

Since a study of this subject became possible only recently, normal heat transport values obviously do not exist. Thus in the subsequent discussion an estimation of variances in the heat transport spectrum was attempted on a monthly basis by referring to the six month averages in fig. 1. Such comparisons cannot be interpreted as representative in view of the sparse data, but are of interest since the degree of spectral variability is thereby suggested.

During the 1959-60 period, which was climaxed by an intense stratospheric warming in January 1960, several major changes in the heat transport spectrum gradually evolved. One such change was the continuous increase of heat transport by wave 1 in the stratosphere from October to January, which then uniformly diminished until the end of the period. Simultaneously as wave 1 increased, the contribution by wave 2 in the stratosphere gradually waned during December 1959, dropping to a minimum in January 1960. In conjunction with these stratospheric events, an opposite spectral pattern appeared in the troposphere during January. That is, wave 1 was a strong transporter in the stratosphere, but appeared less important in the troposphere; wave 2 was a weak transporter in the stratosphere, but was strong in the troposphere. To illustrate more clearly the differences in the heat transport spectrum, values for waves 1, 2, 3 and 4 from tables 1(a), 1(b) and 1(c) were plotted in figures 2, 3 and 4.

The 25-mb average monthly transport values of wave 1 in fig. 2 show a well peaked curve nearly symmetrical for the period about its January maximum, while at 500 mb and 100 mb flattened curves were suggested. A check on the depression of these curves of monthly values was attempted by comparing them with the six month average in fig. 1. Considering fig. 1, the average heat transport by wave 1 at 25 mb for the period was about 100 percent larger than the transport at 100 mb. Whereas the 25-mb January transport by wave 1 shown in fig. 2 was about 200 percent larger than the depressed curve at 100 mb for the same month. Thus for the month of January, wave 1 tends to be weak at 100 mb.

HEAT TRANSPORT WAVE I

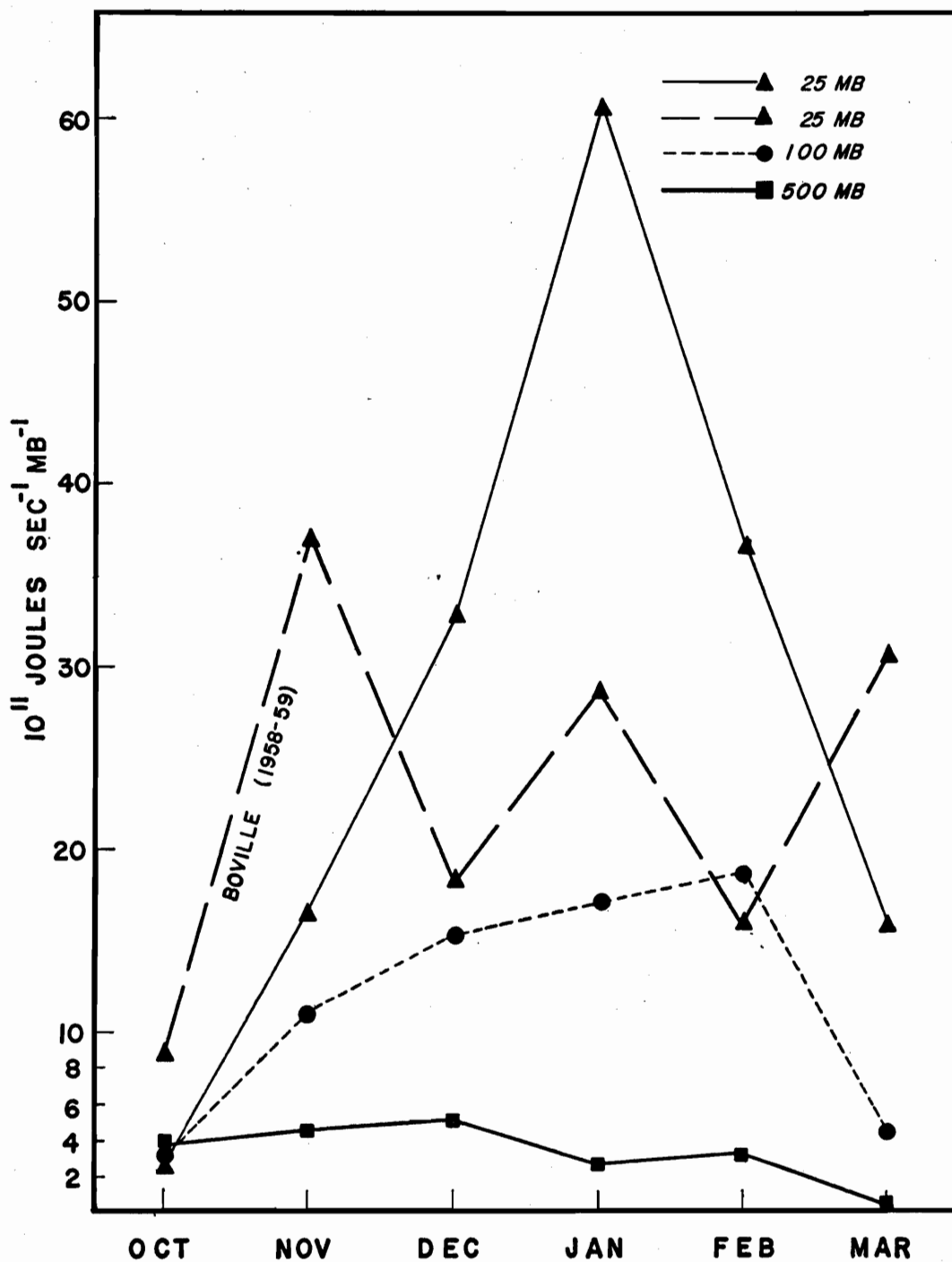


Fig. 2. Graph of monthly heat transport (10^{11} joules sec^{-1} mb^{-1}) by wave one for 500 mb, 100 mb and 25 mb. Dashed curve for 25 mb from Boville (1961).

HEAT TRANSPORT WAVE 2

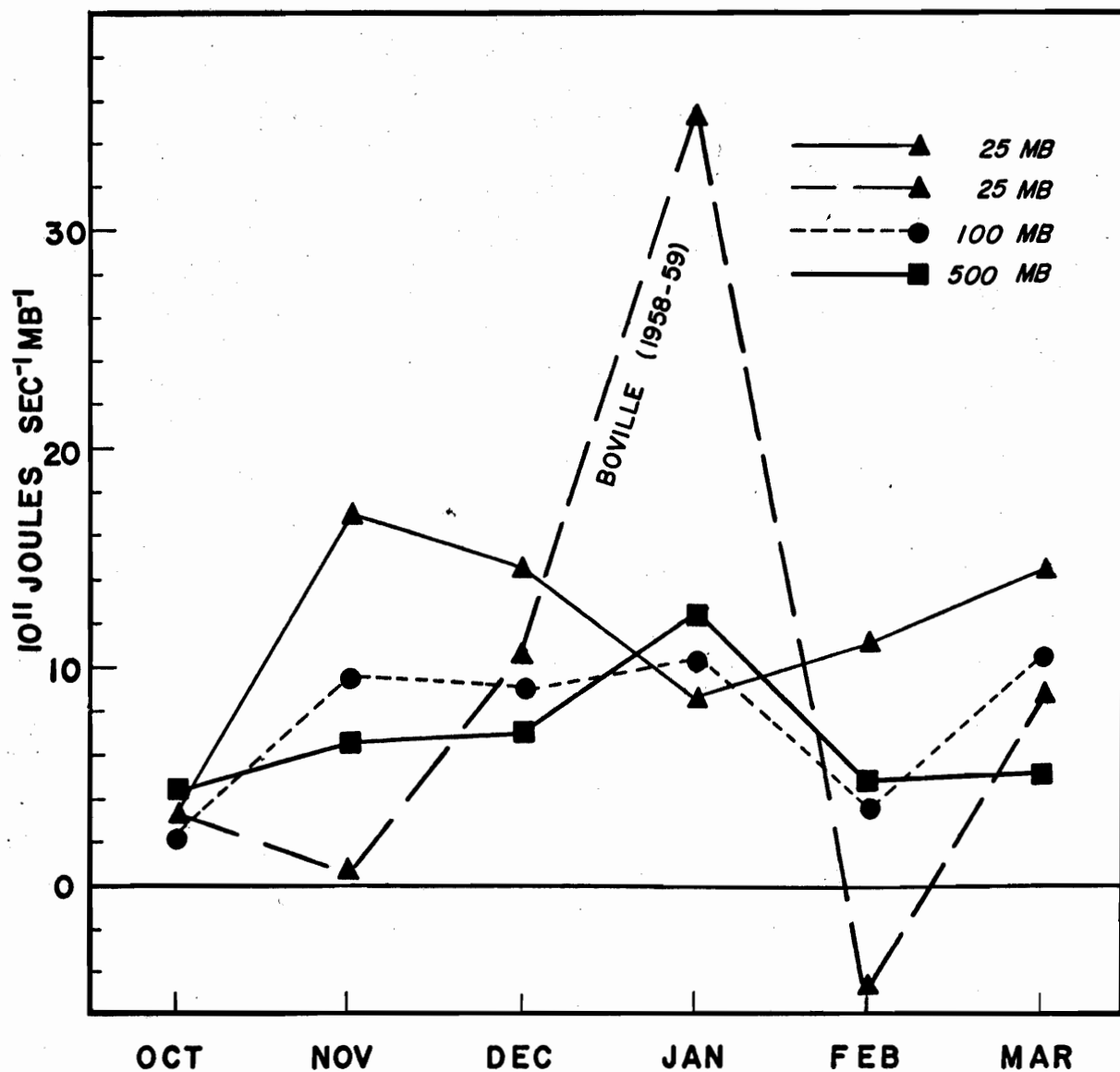


Fig. 3. Graph of monthly heat transport ($10^{11} \text{ joules sec}^{-1} \text{ mb}^{-1}$) by wave two for 500 mb, 100 mb and 25 mb. Dashed curve for 25 mb from Boville (1961).

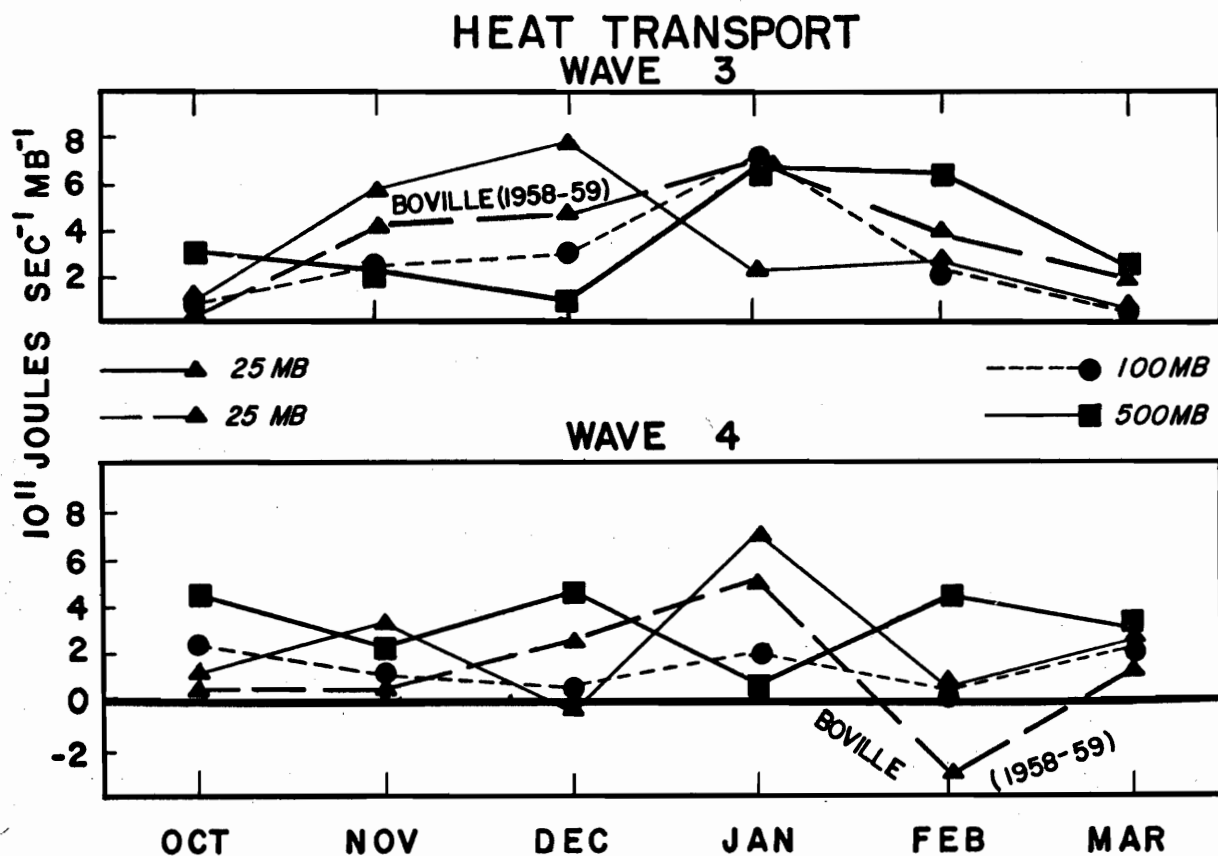


Fig. 4. Graphs of monthly heat transport (10^{11} joules sec^{-1} mb^{-1}) by wave three and four each for 500 mb, 100 mb and 25 mb. Dashed curves for 25 mb from Boville (1961).

However only future studies of other years can verify whether or not this is abnormal. The flattened 500-mb curve of wave 1 in fig. 2 was dismissed as insignificant because of its lack of amplitude. Hence, it appears that as wave 1 became a primary transporter of heat during mid-winter in the stratosphere, its strength did not increase proportionately in the troposphere.

The most salient part of the spectrum was wave 2. As described earlier, fig. 3 shows that it waned to a minimum transport value at 25 mb in January 1960. Surprisingly its 25-mb transport values became less than those at lower levels. Actually at 500 mb wave 2 was the strongest, followed in order by the 100-mb and 25-mb levels. This may imply that wave 2 originated in the troposphere during January 1960. Hence during January 1960, wave 2 contributed only a small quantity of heat to sustain the stratospheric warming. Whereas Boville's (1961) results plotted in fig. 3 show that during January 1959 wave 2 was about three times stronger, as a transporter during this stratospheric warming, than wave 2 in the following year. While during the January 1959 stratospheric warming, wave 2 played the dominant role, followed closely by wave 1. Thus it may be concluded that the January stratospheric warmings resulted mainly from transport by waves 1 and 2 during 1959 and wave 1 during 1960.

For the levels studied (500 mb, 100 mb and 25 mb), waves 3 and 4 contributed relatively little to the heat transport per millibar throughout the period. However a few spectral changes in heat transport appear noteworthy. For instance, in fig. 4, wave 3 at 25 mb shows trends similar to wave 2 for the same level; particularly during

January 1960 when wave 3 was also a weak heat transporter in comparison to lower levels. On the other hand wave 4, like wave 1, became a strong transporter at 25 mb in comparison to the lower levels during this month.

The final warming of March 1959 and March 1960 were not nearly as dramatic as the previously studied January warmings. In both cases the final stratospheric warmings occurred during what could be considered "normal" conditions, that is, in the stratosphere wave 1 was the strongest followed by wave 2, etc. Also during March 1960, the long waves were in all cases the strongest in the stratosphere and gradually weakened at lower levels. Of course, due to the lack of information, a similar analogy cannot be extended to March 1959; but from figures 2 and 3, nothing appears that would contradict this assumption.

Hence it appears logical to assume that during periods of strong heat transport, which produce major stratospheric warmings, the spectrum of this transport may be unique for each case. The discussion of figures 1 through 4 clearly illustrates that the spectrum of heat transport also differs markedly from year to year. These changes of transport between waves 1 and 2, and possibly higher wave numbers, could be due to yearly variations in global heat sources and sinks. Thus it is possible that these long waves are related to world climatic changes.

2.2 Total Northward Heat Transport

In section 2.1 heat transport was studied as a function of wave number and time. From this it was possible to see significant changes in the spectrum as stratospheric events occurred. However it is also

necessary to determine quantitatively how these long waves in toto, contributed to the atmospheric heat budget. This objective is usually accomplished by plotting the net contributions by all waves as a function of latitude and time for a given level, which provides charts of total northward heat transport. With these charts, certain dynamic features of the atmosphere can be approached.

To supplement these charts and others, each 5-day interval of heat transport computations was plotted on graphs as a function of time, wave number and latitude, thus presenting a continuous sequence of heat transport profiles. Such a sequence of graphs was too voluminous for publication, but very helpful in condensing and interpreting these data. They also served as an aid in detecting erroneous data.

As expected, these graphs demonstrated that in the stratosphere the region of strongest transport in waves 1, 2, and 3 was at or north of about latitude 50N. In the troposphere the shorter waves were found south of latitude 60N in the area of baroclinic activity. Occasionally wave 2 at 500 mb appeared relatively strong and persisted at latitudes 60N to 70N. A review of 500-mb constant pressure charts suggest that during these periods of strong northward heat transport, a blocking high pressure system in wave 2 prevailed near latitudes 60N to 70N. Usually there was a strong tendency for these two high pressure systems to retrogress.

The following discussion is based on the total northward heat transport charts in fig. 5. The charts in figures 5(a), 5(b) and 5(c)

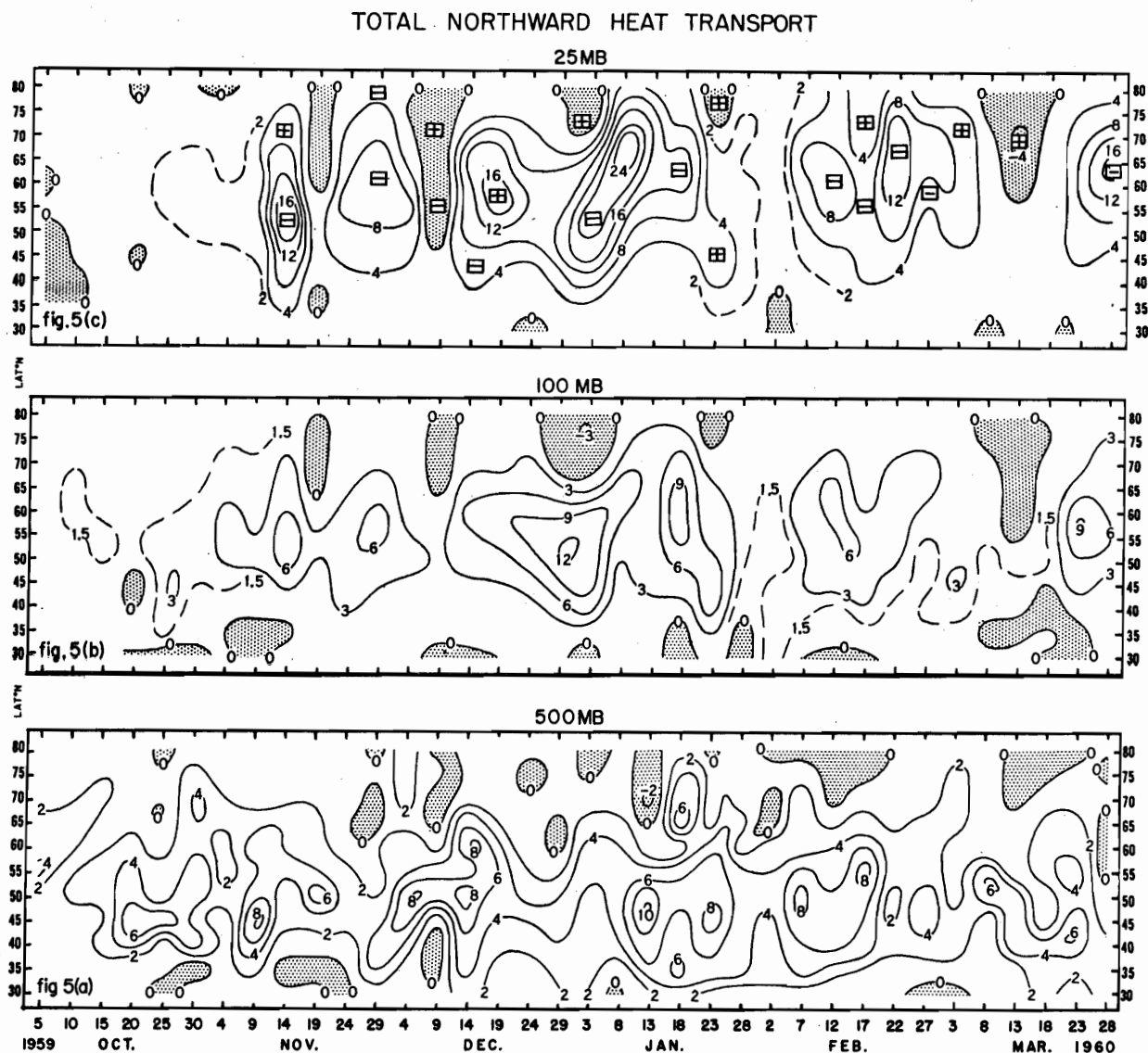


Fig. 5. Total heat transport by waves one through twelve for the period October 5, 1959 through March 28, 1960. Northward transport is positive, southward transport is negative (stippled). Charts (a), 500 mb, at intervals 2×10^{12} ; (b), 100 mb, at intervals 3×10^{12} ; (c), 25 mb, at intervals 4×10^{12} joules sec⁻¹ mb⁻¹. Blocks, \square , in fig. 5c enclose sign of correlation between 25 mb and the 500-mb level shown in fig. 5d.

were constructed by plotting the net contributions of wave 1 through 12 as a function of latitude and time for 500 mb, 100 mb and 25 mb, respectively. A 500-mb heat transport chart by waves 1, 2 and 3 only is included in fig. 5(d) which will later aid in discussing the vertical extent of these long waves. Positive values represent northward transport, whereas negative values indicate southward transport. In most instances, the net contribution by waves 10 through 12 was small. This was probably true at 25 mb, where fig. 5(c) can be compared with Boville's (1961) 25-mb study of waves 1 through 9 for 1958-59 without significant error.

The large scale features of the 25-mb global heat transport in fig. 5(c) were illustrated by a description of strong heat transport that occurred during December 19, 1959 through January 8, 1960. Starting at the first of this period it appeared that the latitude of maximum transport first retreated to lower latitudes with time until the end of the month, then returned to higher latitudes and reached its maximum value on January 8, 1960. In this case, the complete cycle required about 20 days. The pattern that resulted can be largely accounted for by following the action of waves 1 and 2. At this level the strongest transport of heat in wave 1 occurred near latitude 60N to 70N, whereas wave 2 usually reached a maximum north of latitude 50N. Thus varying combinations of these two waves tended to produce a convex trajectory of heat transport as they fluctuated from their mean latitudes with time.

From a study of the integrated total northward heat transport from the surface to 200 mb, Pisharoty (1955) identified northward surges of

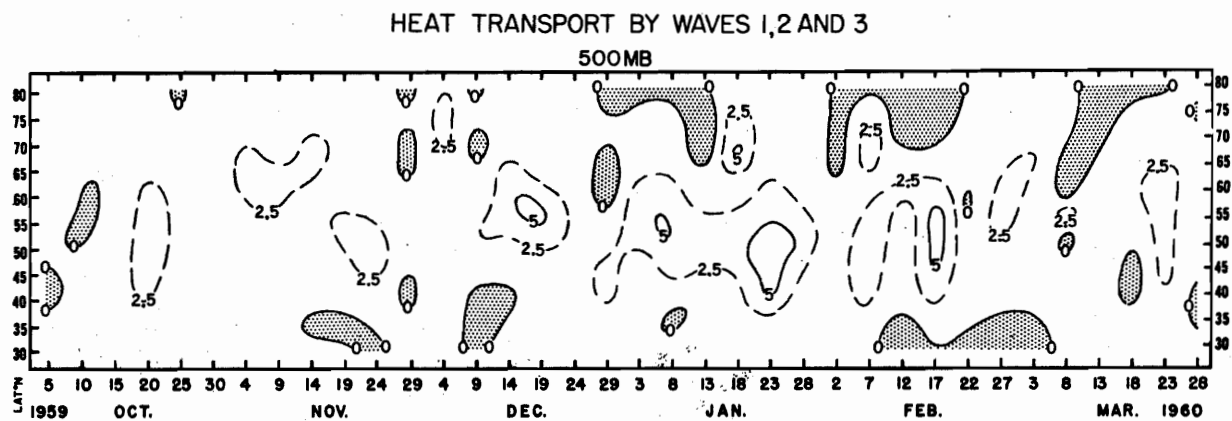


Fig. 5(d). Explanation same as 500-mb chart in fig. 5(a), except transport values are for waves one, two and three only.

heat transport that appear comparable to the final part of the trajectory just described. Accounting for such variations in the spectrum of heat transport was not readily possible, since it is a function of the energy in the eddy flow and the phase relationship between the height and temperature fields. Other similar trajectories, although not as evident, can be identified for dates November 14 through 29, 1959 and February 12 through 22, 1960.

An astonishing aspect of the 25-mb heat transport of fig. 5(c) became apparent when it was compared with fig. 5(e) from Boville's (1961) 1958-59 study. This comparison shows that the occurrence and magnitude of transport events for the two periods were very similar. Note that the 1959 and 1960 January stratospheric warmings discussed earlier occurred within 5 days of each other. Except for the month of March, fig. 5(e) would have been a reasonable forecast of the 25-mb heat transport in fig. 5(c).

At 100 mb the chart of fig. 5(b) revealed a much weaker divergence of heat transport than at 25 mb. However the areas of maximum transport were readily related to those at 25 mb. The transport centers of figures 5(c) and 5(b) for November 14th and 29th appeared nearly vertical, except for a slight northward slope with height. The strong transport centers of December 19, 1959 and January 8, 1960 coincided vertically with the general area of transport, however the correlation of small individual centers was poor. On February 12 thd 22nd the major centers were again closely related.

Although small in magnitude, southward heat transport was in most cases slightly stronger at 25 mb than 100 mb. However this was not

TOTAL NORTHWARD HEAT TRANSPORT AT 25 mb.

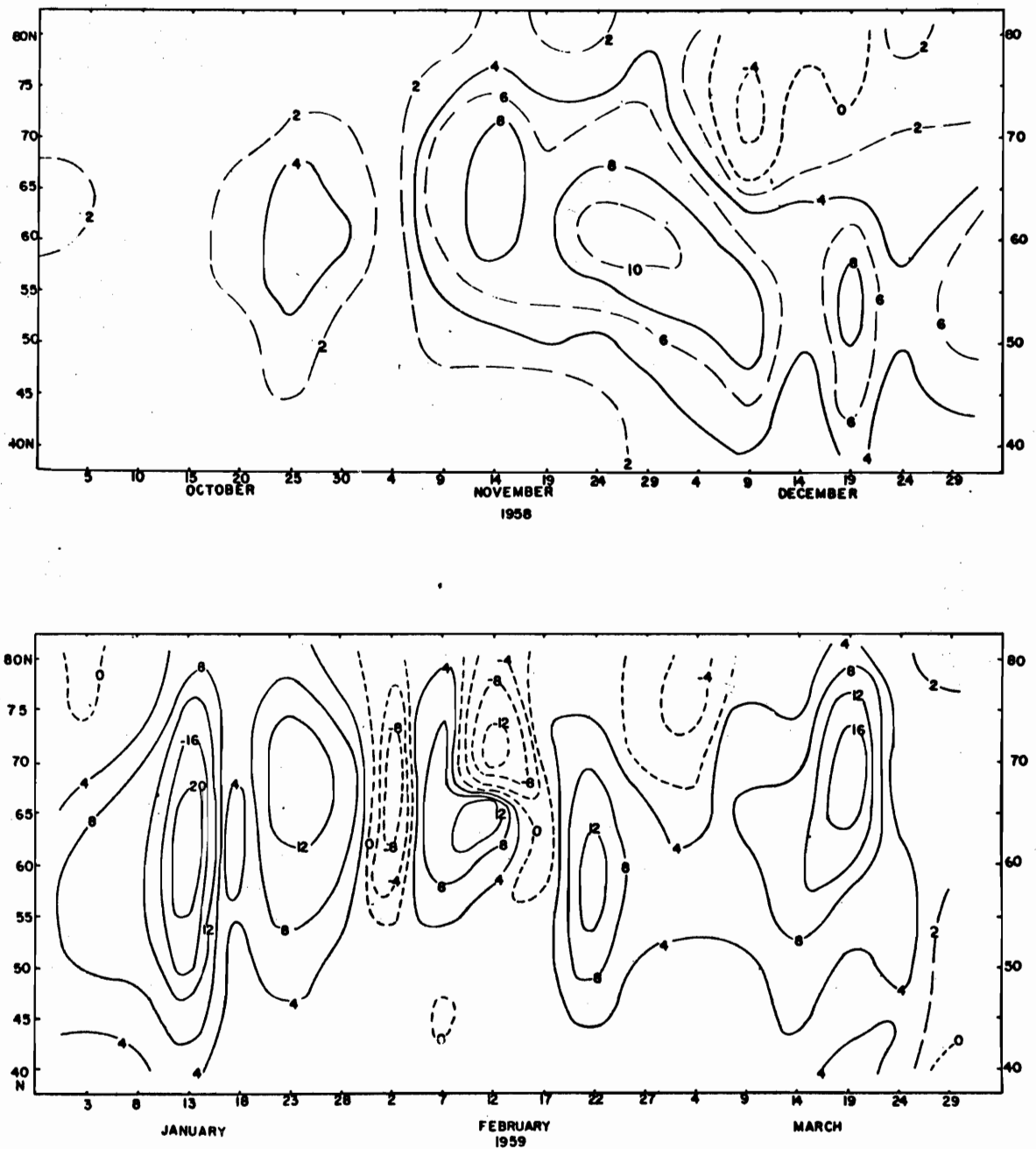


Fig. 5(e). Total heat transport by waves one through nine for period October 5, 1958 through March 29, 1959 at 25 mb. Northward transport is positive, southward transport is negative (10^{12} joules sec^{-1} mb^{-1}). From Boville (1961).

necessarily true for the period of December 29, 1959 through January 3, 1960. During this interval, at latitude 65N to 80N, the 25-mb level (fig. 5(c)) had a minimum of -1.0×10^{12} joules $\text{sec}^{-1} \text{mb}^{-1}$ versus -3.0×10^{12} joules $\text{sec}^{-1} \text{mb}^{-1}$ at 100 mb. These comparisons however must be considered with reservation in view of the 5-day intervals and relatively small quantities measured.

The 500 mb heat transport chart of fig. 5(a) was the most chaotic of the three levels. This was probably due to transport by relatively short lived waves of higher number. As expected the maximum transport was between latitudes 35N and 60N, the region of maximum baroclinic activity. The maximum values on this chart were usually slightly smaller than the upper levels. However the individual centers had stronger gradients, thus producing large, localized divergence values. Decreasing in height from the 25-mb level down to 500 mb, the transport values of the lower latitudes tended to increase in magnitude.

Considering the small density values of the upper atmosphere, it is logical to expect that energy processes at these levels have little influence on the troposphere. However it is possible that the long waves in the Ferrel Westerlies project into the poleward thermal gradient of the polar night westerlies and amplify. Thus in a compressible fluid it may not be possible to a priori separate the two layers.

A comparison of the heat transport chart at 500 mb in fig 5(a) with 100-mb and 25 mb of figures 5(b) and 5(c) revealed that the relationship

of maxima and minima heat transport centers between the troposphere and stratosphere was quite varied. It appeared that the correlation between the two layers was positive or negative for periods of about one month. However, the 500-mb heat transport chart included the waves 1 through 12 and thus may not be comparable with the stratosphere. Also from fig. 1 it appears that about 60 percent of the heat was transported by wave numbers larger than 3. Therefore it is logical to expect distortions in the pattern of the 500-mb transport chart of fig. 5(a), since strong transport by the short waves occur only in the troposphere. On the other hand, it is possible that the analysis of the stratospheric synoptic charts served to filter out the shorter waves if they originally existed in the higher levels.

To check the relationship of the long and short waves in the troposphere, a chart of waves 1, 2 and 3 only (fig. 5(d)) was constructed for 500 mb. Comparing fig. 5(d) with fig. 5(a) showed that the chaotic pattern of total heat transport at 500 mb was in part due to two main sources, that by long waves and/or short waves. In the northern latitudes waves 1, 2 and 3 tended to dominate the 500-mb heat transport. At these high latitudes (above 70N) a positive correlation appeared to exist in most cases between the maxima and minima transport centers of the troposphere and stratosphere. However in most cases at mid-latitudes (50N to 70N) a negative correlation between the two layers was suggested and appeared associated mainly with the long waves. That is, for the more significant cases, the heat transport by short waves was of the same sense as the long waves in the troposphere and

thus served to contribute positively to the total transport. Whereas the short waves had little influence in the higher latitudes throughout the atmosphere, they appeared dominant in several cases at low latitudes (south of 50N). At these latitudes the transports by the shorter waves was traced from the 500-mb to 25-mb level.

The correlations of maxima and minima transport centers between the stratosphere and troposphere were obtained by comparing the 25-mb transport of fig. 5(c) with the 500-mb transport for waves 1, 2 and 3 of fig. 5(d) and the results were indicated in fig. 5(c) as \oplus for positive and \ominus for negative. That is, by this empirical method the vertical correlation of waves 1, 2 and 3 was tested: If the 25-mb heat transport was a maximum and is indicated \oplus , a minimum existed at 500 mb; if the 25-mb heat transport was a minimum and is indicated \ominus , a maximum existed at 500 mb. Likewise for an area indicated \oplus at 25 mb, a corresponding maximum or minimum existed at 500 mb.

At northern latitudes fig. 5(c) shows that positive correlations prevailed except on November 29, 1959 and February 22, 1960. From this presentation of heat transport these negative correlations may be due to two sources; 1.) northward slope of transport maximum, 2.) long waves originating in the upper stratosphere and phased with events of lower levels. The correlation of the strong warming of January 8, 1960 cannot be determined due to the complicated structure during this period. However a comparison of 5(a) and 5(d) suggests that the short waves at 500 mb were transporting in the same sense as the long waves, but did not dominate the transport role.

At mid-latitudes (50N to 70N) the correlation of transport centers was predominantly negative in fig. 5(c). Aside from the period near October 30, 1959 to November 9, 1959 the short waves in the troposphere were not intense enough to change the correlation sign of the two levels. Strong transport throughout the atmosphere by waves 1, 2 and 3 on December 19, 1959 through December 29, 1959 however resulted in a positive correlation, typical of northern latitudes. The beginning of the stratospheric warming on January 3 had a negative correlation and possibly continued through January 8, 1960 at higher latitudes. The best example of negative correlation in fig. 5(c) appeared from February 12 to March 3, 1960. This was also accompanied by a 10 to 15 degree northward slope of the transport centers from 500 mb to 25 mb.

South of latitude 50N, the vertical correlation of transport centers was usually positive due to the shorter waves (that is wave number larger than 3) extending into the stratosphere. However, one case of moderate long wave transport which resulted in a positive correlation was detected. On January 23, 1960 a comparison of figures 5(a) and 5(c) shows that for this case, the long waves at 500 mb were stronger transporters than the short waves. Surprisingly the transport values for this center in fig. 5(d) of 500 mb nearly equals the value of 25 mb in fig. 5(c). Other dates during this period however revealed that the 500-mb short waves were very intense in the low latitudes and were traced to 25 mb. The low latitude transport maxima at 25 mb in fig. 5(c) for dates November 29, 1959, December 14, 1959 and March 23, 1960 were due largely to the intense short waves at 500 mb. On other occasions, November 9, 1959 and January 13 1960,

the short waves were intense at 500 mb but they failed to reach 100 mb of fig. 5(b).

Thus three general classes of vertical structure were defined for heat transport: (1) positively correlated long waves, usually at high latitudes, (2) negatively correlated long waves of mid-latitudes (50N to 70N) with transport by the short waves in the same sense as the long waves in the troposphere, (3) positively correlated short waves in the lower latitudes (below 50N) that penetrated upward to the 25-mb level.

As previously pointed out, good examples of these out of phase relationships of class (2) were observed on February 12 through 22, 1960 in figures 5(a) or 5(d), 5(b) and 5(c). Physically, this negative correlation means that in a baroclinic atmosphere the phase angle between the sinusoidal height and temperature patterns reverse with elevation. That is, if the cold air follows the trough in the height field at lower levels, a large positive heat transport results and in the stratosphere the trough tends to coincide or follow the cold air which produces a zero or negative transport.

How this negatively correlated (class (2)) heat transport structure of the mid-latitudes (50N to 70N) came about was suggested in a multi-level study by Hill (1963). In fig. 6 Hill depicts the daily total heat transport for the period January 12 through 16, 1959. The end of this five day period coincided with a climax of low level cyclonic activity. From this study Hill concluded that there was a level of minimum heat transport in the atmosphere that was displaced

TOTAL NORTHEARD HEAT TRANSPORT

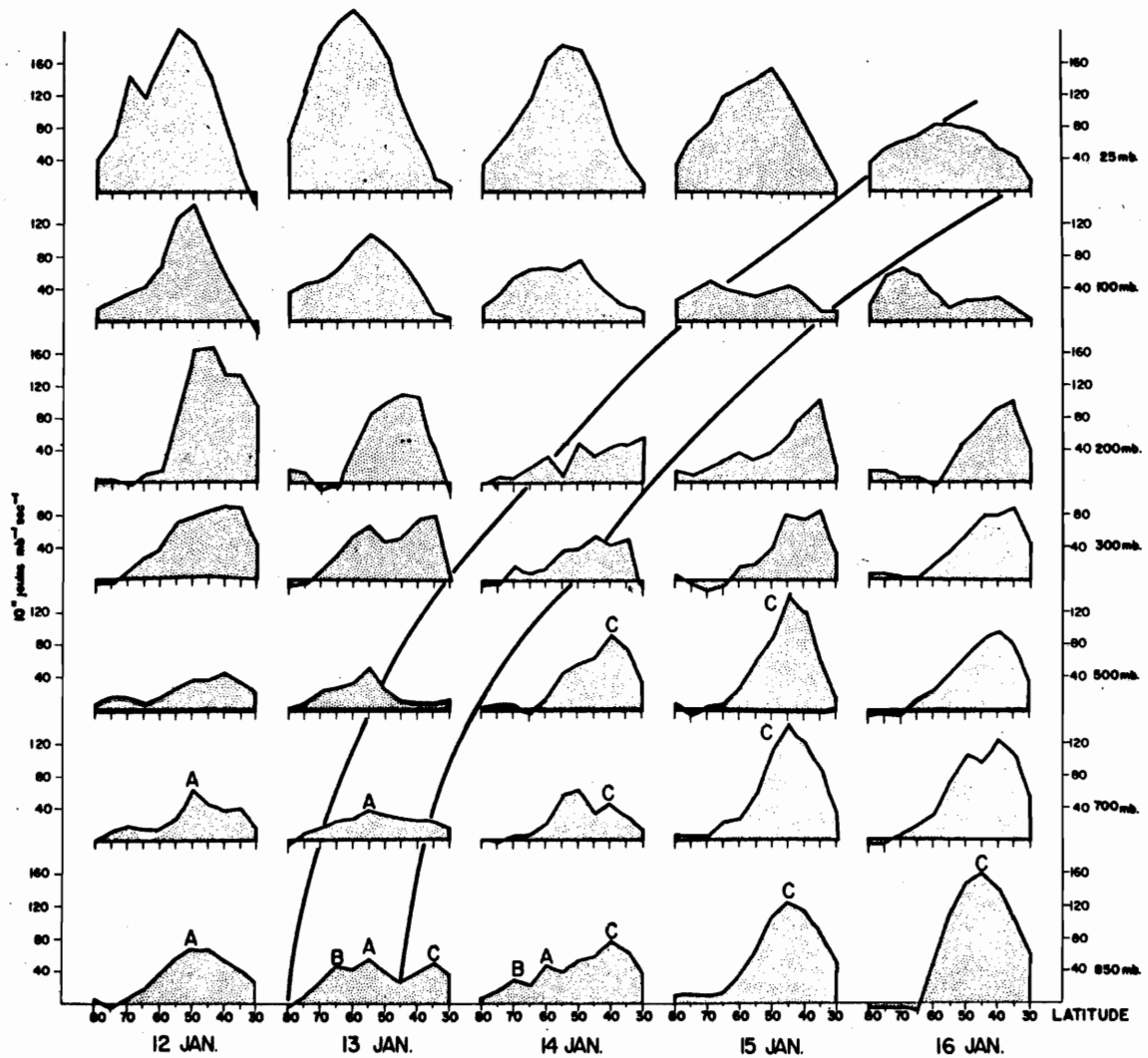


Fig. 6. Total heat transports at all levels for the period 12-16 January 1959. In each cell the total transport is plotted in the vertical and latitude decreases to the right. Heavy curves are a pressure-day locus of minimum transport. A, B and C are maxima which progress northward with time. From Hill (1963).

to higher levels as tropospheric cyclones intensified. Simultaneously the heat transport in the stratosphere decreased to minimum values as the low level development reached its maximum. Little difficulty would be encountered in applying this 5-day study as a model to the cases for class (2) of the mid-latitudes. Note that fig. 6 corresponds with the period January 12 through 16, 1959 in fig. 5(e) from Boville (1961).

From Hill's (1963) study, January 16, 1959, (fig. 6) an example of maximum transport in the troposphere and a minimum in the stratosphere can be seen; while on January 13, 1959 a reverse case existed with a maximum in the stratosphere and minimum in the troposphere. This implies that a level of maximum transport varying in time by about 4 days from the minimum pressure-day locus may exist in the atmosphere. Several examples that fit a maximum pressure-day locus are found in fig. 5, however the final stratospheric warming of March 28, 1960 appears most evident.

Preceding the final stratospheric warming, the heat transport of March 13, 1960 was weak or southward at all levels, except for a narrow band of activity in the mid-latitudes at 500 mb. Actually the stratosphere had been in this state for about 10 days, while in the troposphere weak or southward transport existed mainly in the northern latitudes. During the month of March a gradual latitudinal increase of northward heat transport took place at 500 mb and culminated on March 23, 1960 (fig. 5(a)). A comparison of fig. 5(a) with fig. 5(d) indicated that this activity started in the short waves at about

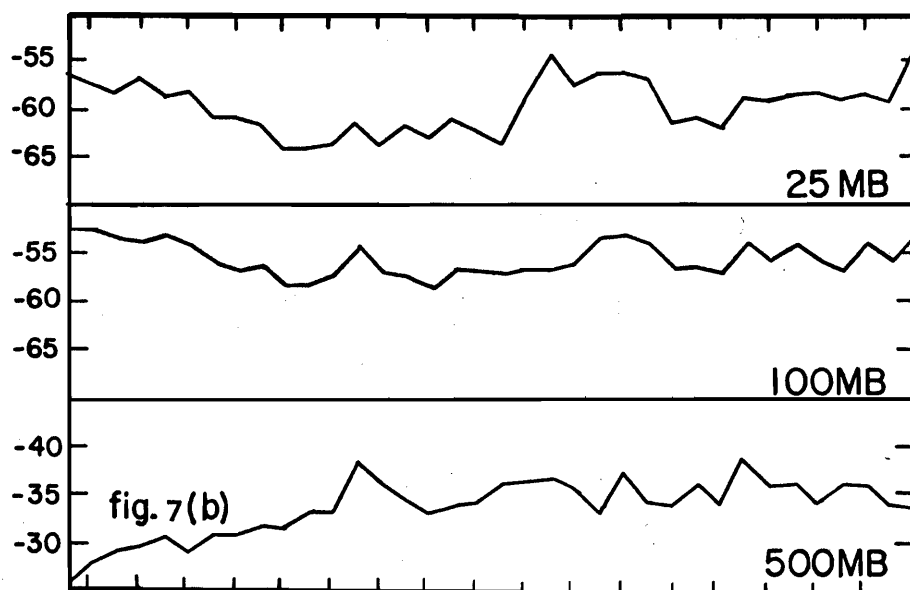
latitude 55N on March 8th and gradually progressed southward until March 23rd. Starting 10 days later, on March 18th, transport by the long waves strengthened until March 23 at about latitude 55N. Thus the long waves were active simultaneously with the short waves during the final warming at 500 mb (fig. 5(a)) on March 23, 1960. Five days later the final stratospheric warming of 1960 was in progress with strong northward transport at 25 mb (fig. 5(c)), while at 500 mb a weak southward transport had developed. The day of maximum northward transport at 100 mb in fig. 5(b) was hard to determine because of the 5-day interval, however it would be easy to adjust the analysis of the heat transport charts of fig. 5 such that the slope would fit the maximum pressure-day locus inferred from fig. 6 of Hill's (1963) study. Thus a reasonable slope of maximum transport was observed from latitude 55N at 500 mb to latitude 65N at 25 mb for the period March 23 to 28, 1960. A similar description of the January 1960 warming is not as straightforward.

2.3 Mean Temperature Changes and Related Atmospheric Phenomena

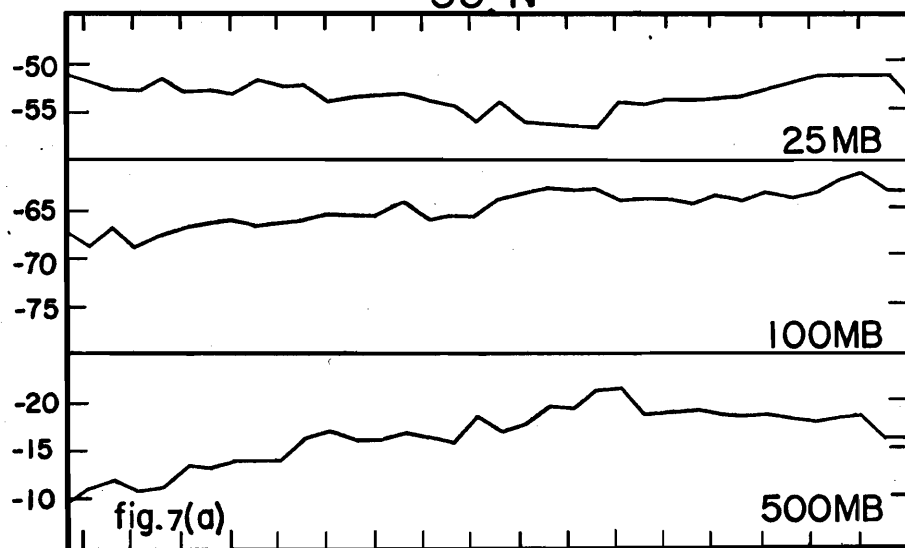
The relation of mean temperature to northward heat transport was examined from a plot of latitudinal mean temperatures computed for the Fourier series. In fig. 7 a selection of these mean temperatures was plotted for latitudes 65N and 35N at 500 mb, 100 mb and 25 mb as a function of time. A comparison of temperature profiles in figures 7(a) and 7(b) with comparable latitudes and levels of heat transport of figures 5(a), 5(b) and 5(c) shows that the January and March stratospheric warmings of 1960 can be followed reasonably well from

TEMPERATURE PROFILES

65°N



35°N



10 20 30 9 19 29 9 19 29 8 18 28 7 17 27 8 18 28
OCT. NOV. DEC. JAN. FEB. MAR.

Fig. 7. Mean temperature ($^{\circ}\text{C}$) profiles at 500 mb, 100 mb and 25 mb from selected latitudes 35N, fig. 7(a), and 65N, fig. 7(b), for period October 5, 1959 through March 28, 1960. Temperature profiles at 500 mb are inverted for comparison with stratosphere. Temperature values were obtained from means computed in the Fourier series.

the mean temperatures. Fig. 7(b) shows that from January 3 to 13, 1960 the 25-mb mean temperature at latitude 65N warmed about 9°C and remained relatively warm throughout the month. During this period, fig. 7(a) shows that the 25-mb mean temperature at latitude 35N cooled about 3°C.

These temperature changes can be accounted for by synoptic events in the stratosphere. From the 25-mb charts of 'An Atlas of Stratospheric Circulation April 1959-May 1960' (McGill University 1962) several of these events are followed. Starting January 3, 1960 a relatively warm high pressure center with air temperatures of -35°C over Korea and northern Japan pushed into eastern Siberia during the following 10 days, which resulted in a general warming of the stratosphere in the northern Pacific region. During its northward excursion this warm air center warmed by subsidence (Craig and Hering 1959), (Boville 1960) and brought temperatures of -30°C into the latitude 70N region, thus accounting for the northern 25-mb warming.

Simultaneously the stratospheric polar night low was centered over north central Asia on January 3, 1960 and began to retrogress. By January 8, 1960 the polar low was over Novaya Zemlya, Russia with a weak cold trough drifting southward over northern China and a second cold trough approaching eastern Canada as it too retrogressed. The trough over China weakened rapidly from January 8 through January 13, 1960 as it filled with warm air, however over Canada the trough intensified and developed a low circulation as it continued to retrogress with the polar low. On January 18th the polar low passed over the northern Norwegian coast and had moved slightly north; while the low in Canada gradually filled over Manitoba, having brought cold air to

most of the middle stratosphere over North America. Hence the heat transports were accomplished by a warm high pressure region moving into the high latitudes and cold lows drifting into the lower latitudes.

Further examination of figures 7(a) and 7(b) suggest that the January warming did not have much influence on the 100-mb level, but occurred mainly in the middle and possibly upper stratosphere. As described earlier, the spectrum of 25-mb heat transport in fig. 2 revealed that most of the heat transport during January 1960 occurred in wave 1, but weakened at 100 mb and below.

As previously pointed out the final stratospheric warming occurred in late March during 1960. However, by late March the atmospheric radiation balance is probably such that any change in the stratospheric circulation would result in a permanent regime of easterly thermal winds due to the lack of a restoring force. In the earlier spectral comparison of the January 1960 warming with the March 1960 warming, the heat transport accompanying the latter was found more uniformly distributed at all levels in waves 1 and 2. This possibly explains why the whole atmosphere responded to the final warming as seen in figures 7(a) and 7(b). An explanation similar to that of the January warming also accounts for the final stratospheric warming.

The above qualitative discussion pointed out several interesting synoptic features, however there is no measure of how effective the heat transport was in heating the atmosphere. Aside from heating the atmosphere, it is possible that this heat transport was coupled with other thermodynamic processes; 1) vertical transport of heat,

2) adiabatic vertical motion, 3) release of latent heat at tropospheric levels, 4) fluctuations of the atmospheric radiation balance. An individual evaluation of these parameters was not attempted, however the net contribution can be derived from the consideration of atmospheric temperature changes due to divergence of the heat transport and the change of mean atmospheric temperatures.

2.4 Divergence of Heat Transport and Mean Temperature Changes

The quantity of heat available to the atmosphere by a "so called" warming is a function of the divergence of northward heat transport. From this calculated quantity of heat the expected temperature change is readily computed. The mean temperatures obtained from the Fourier series analyses were used to compute the observed rate of temperature change. Hence for a conservation of energy, any difference between the expected temperature change and the observed temperature change must be balanced by the net effect of the four previously listed thermodynamic processes.

Several additional charts are necessary before the net contribution of these processes can be evaluated. The mean temperatures of the Fourier series are plotted as a function of latitude and time for 500 mb, 100 mb and 25 mb and appear in figures 8(a), 8(b) and 8(c), respectively. (Note that the profiles of fig. 7 are of the same data source). Several interesting features of the atmosphere were observed when these three mean temperature charts were compared with the heat transport charts of fig. 5.

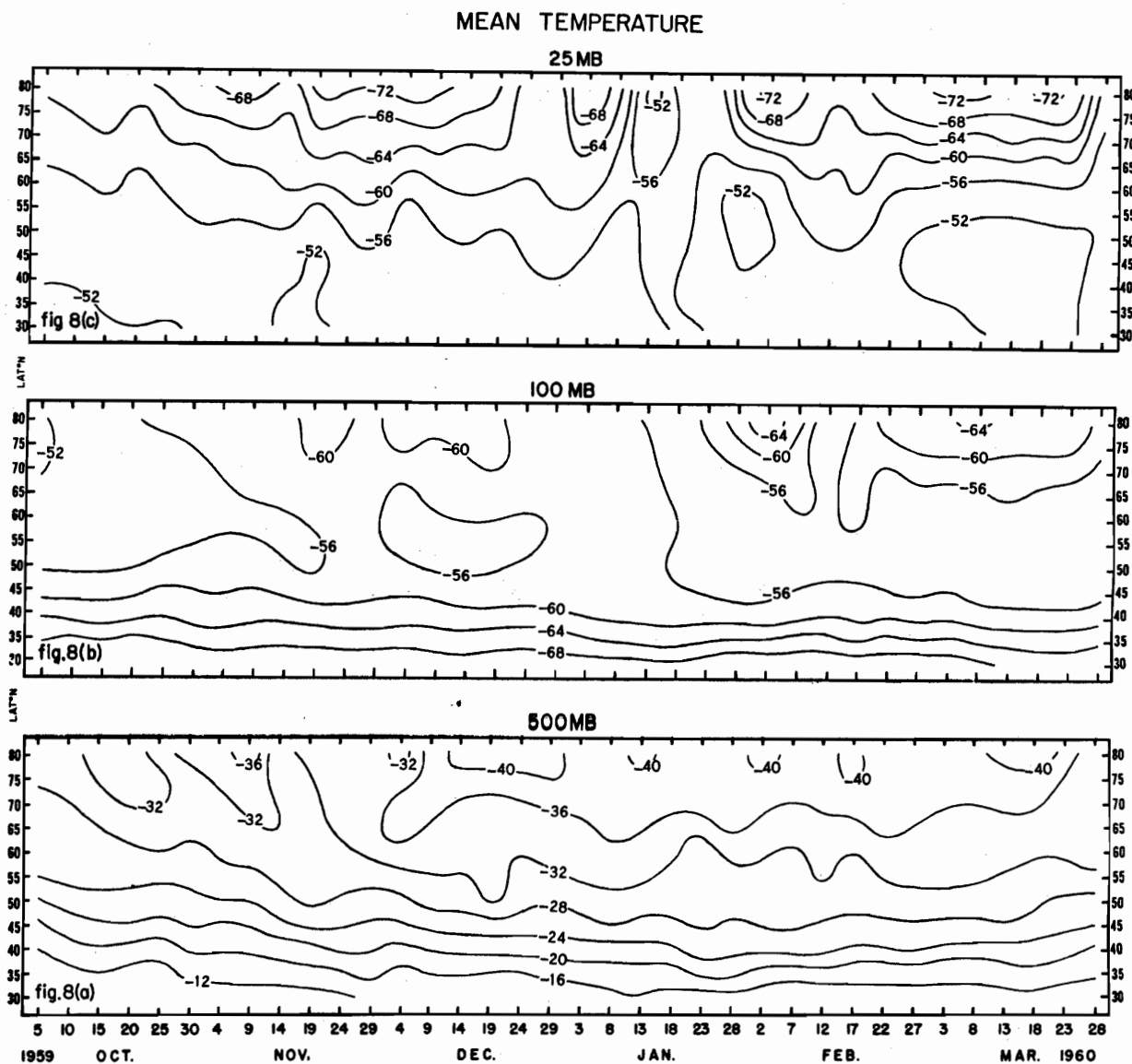


Fig. 8. Mean temperature ($^{\circ}\text{C}$) charts for period October 5, 1959 through March 28, 1960. Charts (a), (b) and (c) are the 500 mb, 100 mb and 25-mb levels respectively. Temperature values were obtained from means computed for the Fourier series.

North of latitude 50N, 25-mb temperature changes of large magnitude were found at nearly all latitudes. Fig. 8(c) shows that these large 25-mb temperature changes take place from December 24, 1959 to February 12, 1960 and again at the end of March 1960. Aside from these large cellular features, the temperature gradient, $-\nabla T$, was directed generally toward the North Pole. These large temperature changes at 25 mb appeared associated with strong heat transports.

The 25-mb temperature chart of fig. 8(c) also reveals large scale temperature patterns in which the isotherms diverge or converge for a given day. These thermal patterns also correspond with heat transport and at times extend from latitude 40N to polar latitudes. Examples of these are found on November 19, 1959 and February 12, 1960; the first occurred during southward transport (fig. 5(c)), while the latter was a case of strong northward transport. Thus as implied, a cooling occurred at high latitudes and a warming took place in lower latitudes on November 19th as heat was transported southward.

February 12, 1960 was the reverse situation and is the best example of a divergent temperature pattern. In this case the northward transport (fig. 5(c)) was clearly extracting heat from the low latitudes and creating a warming at high latitudes. Other similar, but smaller scale, features in the mean temperature field can be likewise described. These features were less defined at lower levels and thus they appear to be characteristic of the middle stratosphere.

At 100 mb the mean temperature chart in fig. 8(b) shows three distinct temperature features: 1) a strong uniform low latitude equatorward temperature gradient, 2) a broad zonal warm belt at mid-latitudes and 3) cellular temperature patterns of moderate intensity in the northern latitudes. South of latitude 45°N was a region with $0.7^{\circ}\text{C}/\text{lat. deg.}$ equatorward temperature gradient, $-\nabla T$. This gradient existed because north of this latitude the tropical tropopause vanishes and the atmosphere becomes a relatively warm barotropic region, thus establishing a strong temperature gradient in the lower latitudes with colder temperatures in the equatorial regions.

The warm region at latitudes 50°N to 60°N of fig. 8(b) is commonly called the stratospheric warm belt. It is usually a barotropic region that exists between the Ferrel westerlies and the westerlies of the polar night low. Depending upon the position of these westerly currents, this region of relatively warm air, -50°C to -55°C , can extend northward into polar latitudes during stratospheric warmings.

At higher latitudes, north of the stratospheric warm belt, the 100-mb heat transport (fig. 5(b)) appears related to most of the cellular temperature patterns. Usually these patterns at 100 mb were less intense than the related pattern at 25 mb. For this period the mean 100-mb temperatures of fig. 8(b) ranged from -54°C to -66°C in the polar regions. In most cases the 100-mb and 25-mb events appeared related.

The 500-mb mean temperature chart suggested only two temperature regimes. The main feature of the 500-mb temperature chart in fig. 8(a)

was the seasonal variation in differential radiational heating of the atmosphere. This heating contributes mainly to maintain a temperature gradient also of about $0.7^{\circ}\text{C}/\text{lat. deg.}$ in the lower latitudes. During October this temperature gradient extends from the equatorial regions up to latitude 60N , then drops to about latitude 50N in the winter months. This region showed little response to heat transport.

In the northern latitudes fig. 8(a) shows that, outside the region of strong, low latitude temperature gradient, the 500-mb temperature gradient was weak and irregular with cells of temperature maxima and minima. These 500-mb mean temperatures ranged from -32°C to -44°C and appeared weakly related to the heat transport chart of fig. 5(a). During periods of broad scale changes, about 10 days or longer, temperature fluctuations occurred in response to the heat transport.

Within the latitude zone of 50N to 70N several temperature changes of about 5°C exist. An attempt to account for these temperature changes by comparing the chaotic transport pattern of 500 mb with the relatively simple 500-mb mean temperature field resulted in several unaccountable singularities. However a comparison of the 500-mb mean temperature chart of fig. 8(a) with the heat transport chart for waves 1, 2 and 3 only in fig. 5(d), revealed that these small changes in the mean temperature field were probably due to long wave heat transport. Possibly this long wave phenomenon could also be detected at 100 mb if the short waves were similarly filtered from the total heat transport values. However the mean temperature changes in the mid-latitude belt at 100 mb (fig. 8(b)) are smaller than those of the 500-mb temperature chart

fig. 8(a)). Hence if the 100-mb heat transport and 100-mb temperature field were compared, the 5-day interval of this study probably would be too crude to obtain reliable results.

The horizontal divergence of heat transport, $\text{div}_2 H_T$, was determined from charts of total northward heat transport in fig. 5. The $\text{div}_2 H_T$ was accomplished by a 5° latitude displacement of H_T values northward and computed for 1-day interval, which is expressed as ΔH_T . The charts of fig. 5 must be corrected for northward convergence of area and this was included in the divergence computations. From the thermodynamic expression for heat transfer per unit mass

$$\Delta H = C_p \Delta T \quad C_p = \text{specific heat at constant pressure}$$

it follows that

$$\frac{\Delta T}{\Delta t} = \frac{0.03 \times 10^{-12}}{\sin \phi_2 - \sin \phi_1} \Delta H_T \quad ^\circ\text{C per day} \quad (5)$$

where $\sin \phi_2 - \sin \phi_1$ is the northward latitude shrinkage term at 5-degree intervals. Thus $\frac{\Delta T}{\Delta t}$ is the temperature change expected for one day of heat transport. These divergence values for 500 mb, 100 mb and 25 mb are shown in figures 9(a) or 9(d), 9(b) and 9(c) respectively, and were obtained by computing point values. In fig. 9 the convergence of heat transport is shown as positive, while divergence is indicated as negative. The chart of fig. 9(d) was constructed from the heat transport chart of fig. 5(d) which is for waves 1, 2 and 3 only.

Having developed an expression to determine the expected change of temperature, the actual change can be readily arrived at by determining $\frac{\Delta \bar{T}}{\Delta t}$ of the mean temperature, \bar{T} , charts in fig. 8. The

DIVERGENCE OF TOTAL NORTHWARD HEAT TRANSPORT

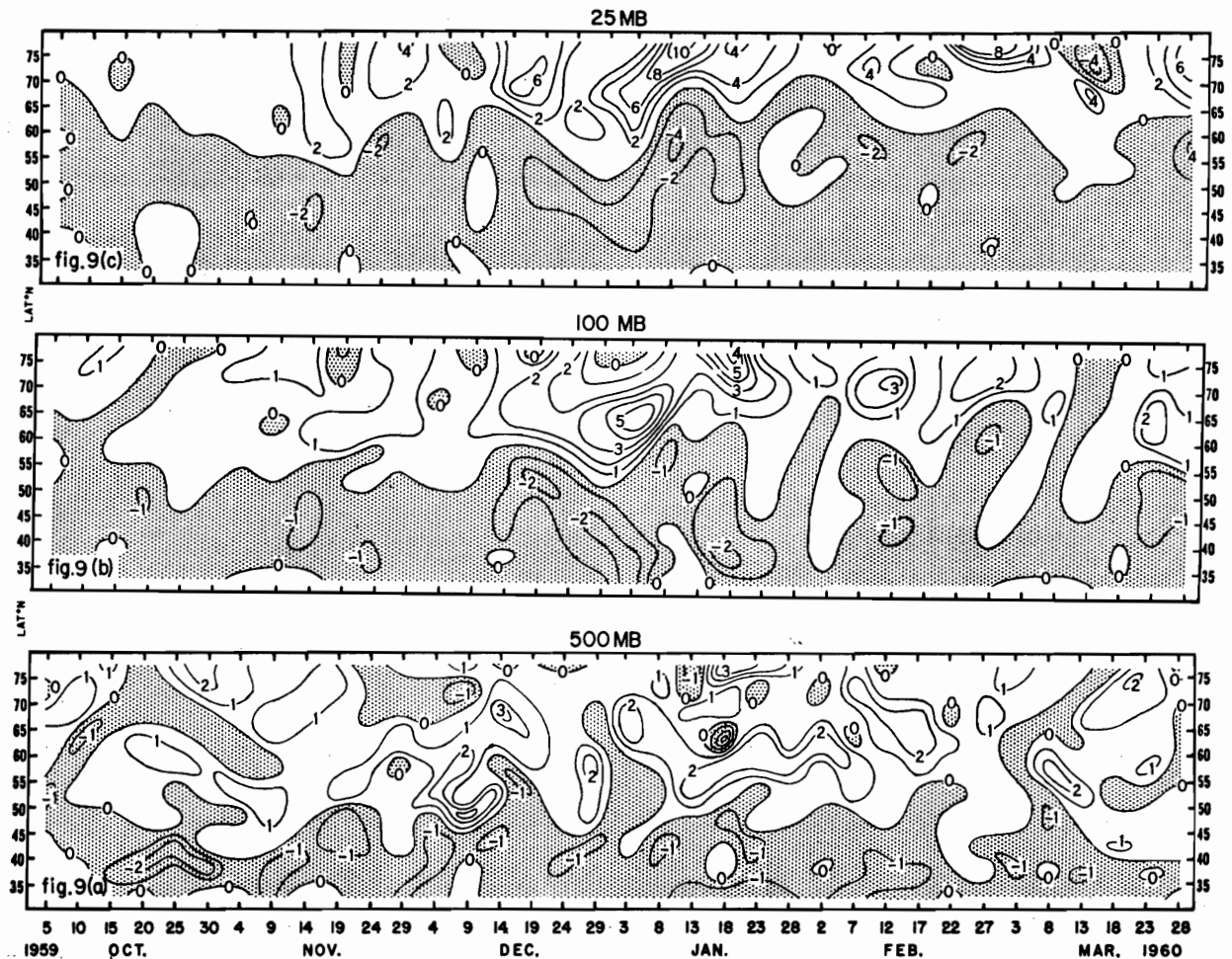


Fig. 9. Calculated temperature change charts for $^{\circ}\text{C}$ per day computed from time derivatives of the divergence of total heat transport for period October 5, 1959 through March 28, 1960. Charts (a), (b) and (c) are the 500 mb, 100 mb and 25-mb levels respectively, for waves one through twelve. Areas of convergence are positive and divergence are negative (stippled).

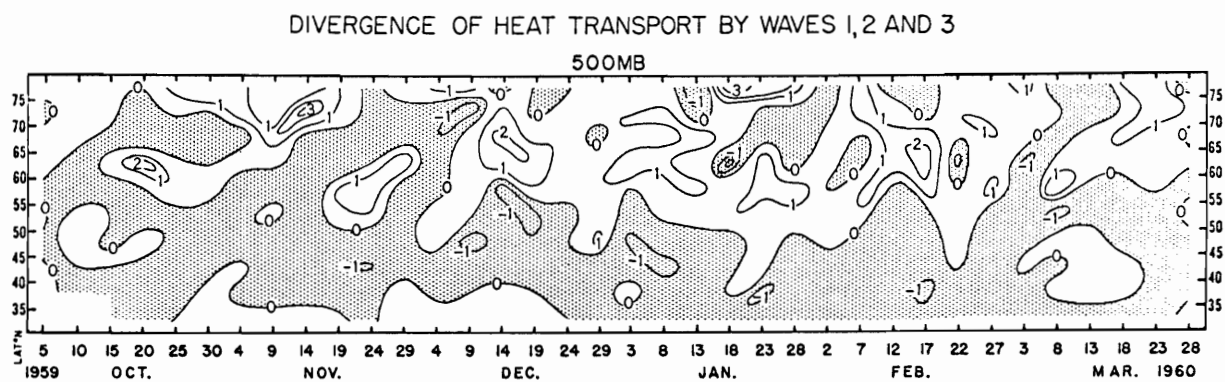


Fig. 9(d). Explanation same as fig. 9(a), except computations are from 500-mb heat transport chart in fig. 5(d).

actual mean temperature change was determined graphically from \bar{T} fields of each respective level (500-mb, 100-mb and 25-mb). These charts were not published. Hence the difference of the computed (fig. 9) $\frac{\Delta \bar{T}}{\Delta t}$ and actual mean temperature changes (or $\frac{\Delta T}{\Delta t} - \frac{\Delta \bar{T}}{\Delta t}$) at each level (500-mb, 100-mb and 25-mb) gives a quantitative measure of the other thermodynamic processes which must act if this difference is non-zero. These charts of heat transport "budget" were analyzed for 500 mb, 100 mb and 25 mb and appear in figures 10(d), 10(b) and 10(c), respectively, units are in $^{\circ}\text{C}$ per day. That is, fig. 10 shows that for an existing heat transport, a dissipation of heat is required in positive regions and heat must be added in negative regions in order to maintain the observed mean temperature changes.

At 25 mb (fig. 10) rather large plus and minus values were observed as a result of heat transport and must be accounted for. One possible source of heat loss in the winter stratosphere is terrestrial radiation. This however appears insignificant compared to the magnitude of the values in fig. 10(c). Most authors (Ohring 1958, Murgatroyd and Goody 1958 and others) find cooling rates of about 1°C per day.

The release of latent heat in the stratosphere is also insignificant. In the troposphere however it probably contributes considerably at times and should be included in this type of study. But since the original intention of the author was a treatment mainly of the stratosphere, the latent heat problem is dismissed as beyond the scope of this study.

HEAT TRANSPORT "BUDGET"

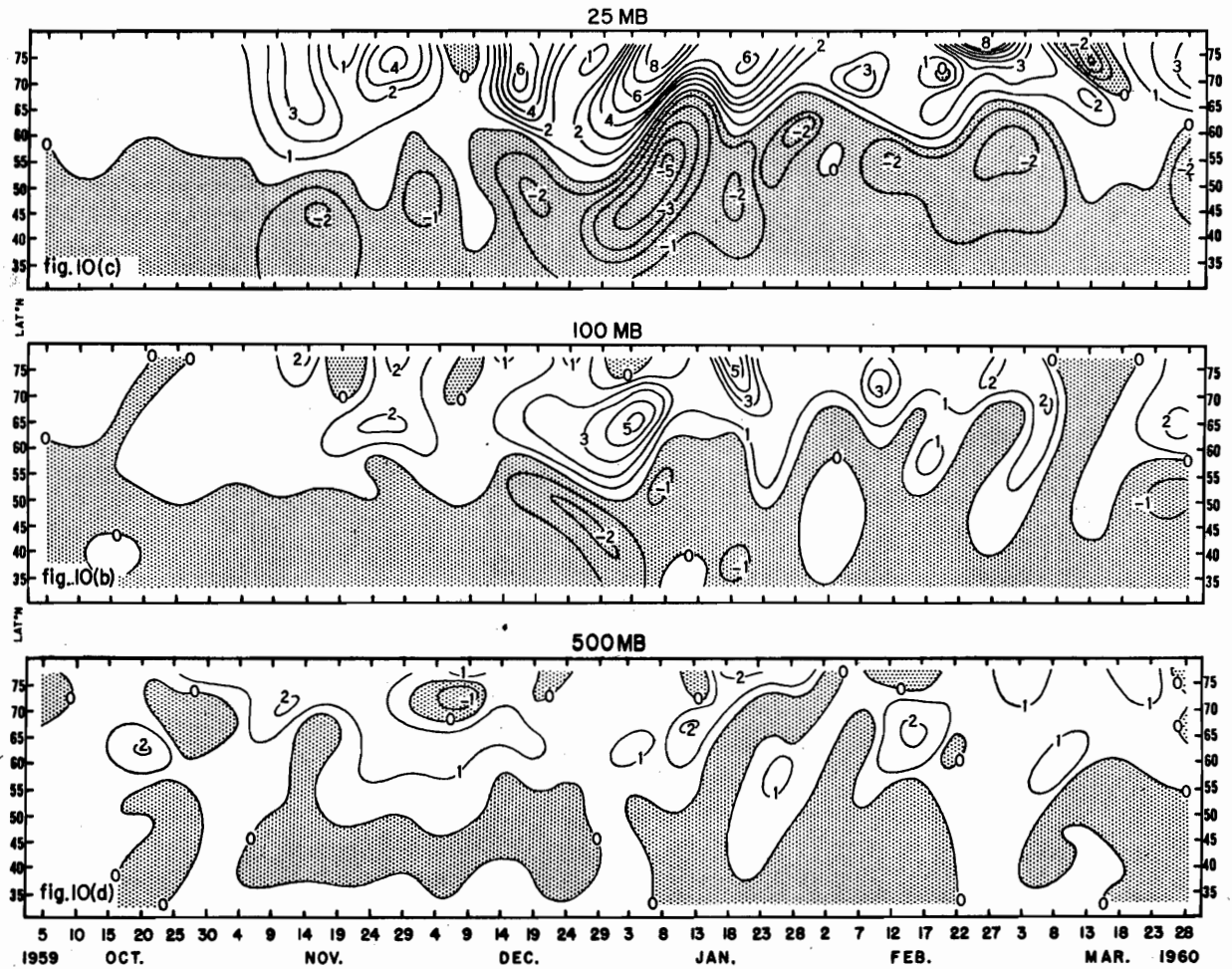


Fig. 10. Heat transport "budget" charts ($^{\circ}\text{C}$ per day) for period October 5, 1959 through March 28, 1960. Chart (d) is the 500-mb level for waves on, two and three. Charts (b) and (c) are the 100-mb and 25-mb levels respectively, for waves one through twelve. (Stippled area negative)

Part of this heating difference may be the result of vertical heat transport due to the covariance \overline{Tw} where w = vertical velocity. But this term is difficult to ascertain and is probably small in view of the nearly isothermal lapse rate in the winter stratosphere.

The most likely explanation is adiabatic vertical motion. Teweles (1963) found from vertical motion calculations that the winter stratosphere had relatively strong ascending motions in the polar regions. He therefore concluded that if the radiation losses were small, there must be strong northward heat transport into this region to support the calculated positive vertical motion. These findings by Teweles are in agreement with this study, if adiabatic vertical motion is considered the primary means of balancing the heat transport "budget". In view of the information available, vertical velocities are assumed the necessary mechanism to explain the differences between the expected temperature changes and the observed mean temperature changes as given in fig. 10. Mean ascending motion in the polar winter stratosphere is contrary to the meridional circulation suggested by Murgatroyd and Singleton (1961).

2.5 Stratospheric Vertical Motions

The previous discussion of heat transport and mean temperature change has implied that these atmospheric parameters were closely related in the long waves. The degree of this correspondence was the largest in the stratosphere. It appears that vertical motions were also associated with heat transport and temperature change, thus serving as an important mechanism that contributed to stratospheric temperature changes.

From fig. 10(c) it is evident that large organized fields of plus and minus isopleths of $^{\circ}\text{C}$ per day existed at 25 mb, which was assumed to represent mainly vertical motion patterns. A comparison of these values at 500 mb, 100 mb and 25 mb of fig. 10(d), 10(b) and 10(c) respectively, shows that the stratosphere contained the strongest of these fields. These values are in turn more meaningful if converted into vertical motion values. Hence, from the adiabatic lapse rate of 9.8°C per km and assuming a radiation loss of 1°C per day for the northern latitudes, the 8°C per-day isopleth of the heat budget chart in fig. 10(c) represents a vertical velocity of 1 cm per sec. Since this is a linear relationship, the charts in figures 10(d) and 10(b) for the 500-mb and 100-mb levels, respectively, can be likewise converted to fractions of vertical motion in cm per sec.

In terms of vertical motion, the heat budget chart of fig. 10(c) suggests that the stratosphere was influenced by periods of alternating cells of meridional circulation. Comparing the 25-mb heat budget chart of fig. 10(c) with the mean temperature chart of the same level of fig. 8(c) indicated the important role vertical motion had in the stratosphere. It appears that the vertical motion can act to either inhibit or reverse the temperature changes due to heat transport at 25 mb.

From early November 1959, until the first part of December 1959, the high latitude meridional cells at 25 mb alternated in direction of circulation and at the same time served to dampen the temperature change that should result from the heat transport. That is, as heat was transported northward over the globe, subsidence occurred in the

southern latitudes, coupled with positive vertical motion in the northern latitudes. For southward transport the converse description applies. Hence fig. 9(c) shows that during these events the warming occurred with convergence of heat transport and divergence of heat transport resulted in cooling.

However it appears that the vertical motions of the stratosphere can vary with respect to the thermal field. This became noticeable in mid-December, 1959 and continued throughout the period. During the period of December 14 through 19, 1959, the 25-mb heat budget chart of fig. 10(c) shows ascending air of about 0.5 cm per sec at latitude 70N. From fig. 8(c) it was evident that the 25-mb mean temperature rose only slightly. However the vertical velocities subsided after December 19th and it was then that the 25-mb mean temperatures of fig. 8(c) showed a high latitude warming that occurred through December 24th. Note that in previous cases, the warming occurred during strong convergence of heat transport (see figures 5(c) and 9(c)) accompanied by ascending air.

In a second example, during the stratospheric warming of January 1960, the vertical motion appeared to lag the heat transport. In fig. 10(c) what appears to be a stratospheric meridional circulation started from low latitudes on December 24 to 29, 1959 and moved northward until mid-January, 1960. A suggested schematic representation of this meridional cell for January 8, 1960 is shown in fig. 11. Comparing the 25 mb heat budget chart in fig. 10(c) with the mean temperature in fig. 9(c), the origin of this cell was found to be the type described during November through early December. However it appears that this

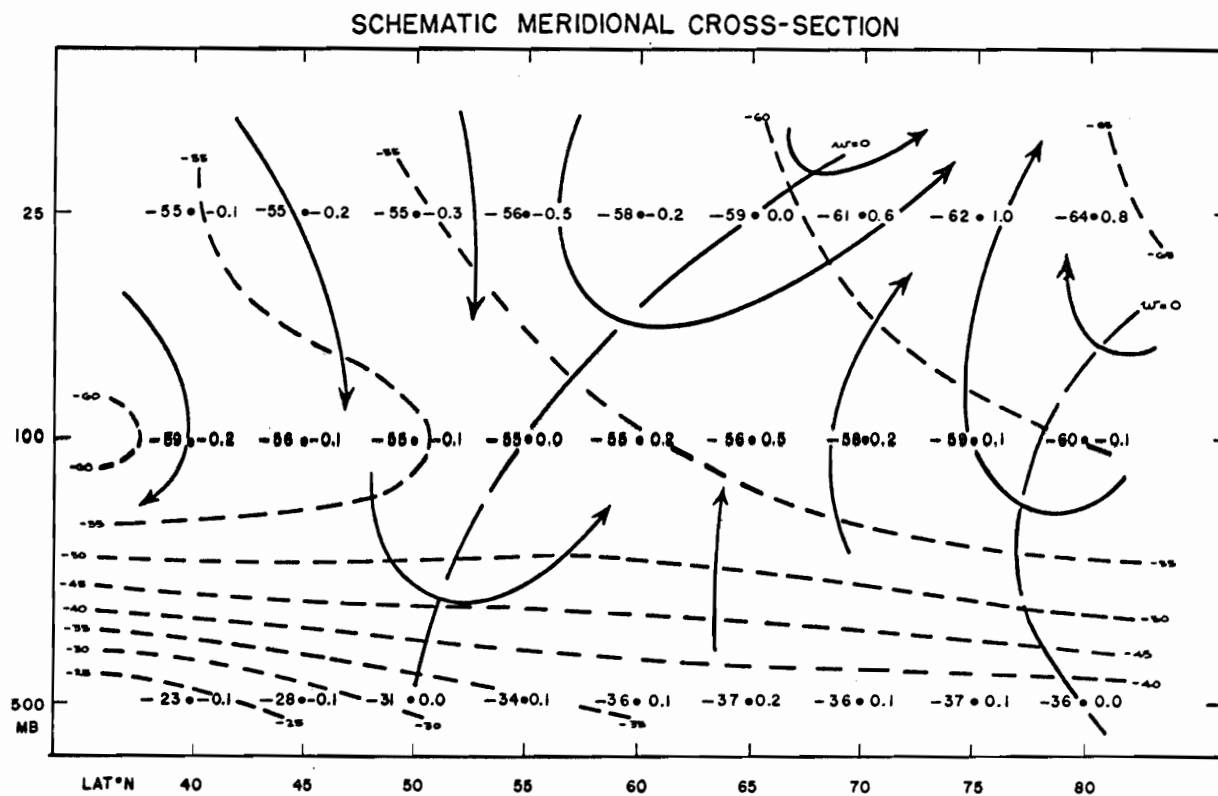


Fig. 11. Schematic cross-section of temperature and streamlines of vertical motion for January 8, 1960. Temperatures, °C, on left (dashed lines) and vertical motion, cm sec^{-1} , on right (solid lines represent meridional flow) of each point.

pattern switched in early January 1960 and as it moved northward became similar to the circulation during December 14 through 24, 1959, whereby the ascending air produced a net cooling in the early stages of the strong heat transport. The strongest 25-mb positive vertical motion of about 1 cm per sec was reached about 5 days before the warming culminated. Although the maximum subsidence of about 0.5 cm per sec was reached earlier, simultaneously with the maximum ascending air, the final warming at the high latitudes occurred in regions of subsidence or weak positive motion.

This phenomenon was accounted for by comparing the divergence chart of fig. 9(c) and heat transport chart of fig. 5(c) with the vertical motions of fig. 10(c). These charts indicate that both the warming and meridional circulation were dissipating. However, it appears that the warming reached the observed peak intensity because the meridional circulation was waning more rapidly than the rate of heat transport. Throughout the remainder of the period, this same pattern of vertical motion and temperature change was the usual case in the stratosphere. The exact nature of the final stratospheric warming in March 1960 could not be determined since it falls at the end of the period studied, however it probably follows the same course of events as the January 1960 warming.

Although the function of the vertical motion was found to differ with respect to temperature change, the centers of maximum positive vertical motion continued to correspond with the areas of maximum

convergence of heat transport. Thus in view of the variations found between vertical motions and temperature changes at 25 mb, it appears that the subject is worthy of further study and may shed added light on the dynamics of the stratospheric warmings.

The 25-mb heat transport at high latitudes during February 22 through 27, 1960 appeared to be an unusual case. The divergence chart of fig. 9(c) shows that heating for this period was the most intense near latitudes 75N to 80N. However, the mean temperature chart for this level in fig. 8(c) shows a slight cooling in this region. From the heat budget chart of fig. 10(c) this was accounted for by strong positive vertical motions that exceeded 1 cm per sec. Thus during this interval of strong heat transport, the net result was a cooling in the region of strong convergence due to large ascending motion of air.

General features of the stratosphere show that the polar night air was usually ascending, interrupted only occasionally by slowly subsiding air. At times, 5-day to 10-day periods of major upward motion developed in which the mean motion of the air attained 1 cm per sec.

South of latitude 60N the 100-mb and 25-mb charts of figures 10(b) and 10(c) respectively, have mainly negative values; indicating that additional heat was required to account for the observed temperature changes. However, radiational heating probably contributes largely to the required heat balance and thus vertical motions south of latitude 40N are undeterminable. The region of largest negative values

occurred near latitudes 50N to 60N, which was directly over the stratospheric warm belt of the lower stratosphere. This belt of 25-mb subsidence at these latitudes extended to lower levels and was probably related to the persistent warm belt seen in the 100-mb mean temperature field of fig. 8(b). At 100 mb, fig. 10(b) shows that the regions of strong subsidence from higher levels were well dampened in the lower stratosphere.

A continuous warm belt was not detected at 25 mb, possibly because the strong heat transport at this level was of greater magnitude than the heating due to subsidence and thus tended to obliterate this phenomenon at higher elevations. However beginning in mid-January, fig. 8(c) shows that a broad warm belt developed at 25 mb and existed through March. This partial 25-mb warm belt was located at about latitude 45N, which is 10 degrees of latitude south of the 100-mb warm belt. This implies that, for the period studied, the mean thickness of the subsiding layer in this region of the stratosphere was thicker during mid-January through March than October through mid-January.

This correspondence of vertical motion and temperature change in the stratosphere extended down to the 100-mb level for only the cases of strong vertical motion. For the most part, the correspondence found at 25 mb was still true at the 100-mb level, however, a comparison of figure 10(c) with 9(c) suggested that several distortions existed in the 100-mb heat budget chart. This was probably due to the influence of short waves (four and smaller) extending up from the troposphere.

Earlier it was shown that the correspondence between the 500-mb heat transport and mean temperature changes of this level was possible by restricting the heat transport values to the long waves. However this technique gave poor results when applied in relating the vertical motion (fig. 10(d)) and mean temperature changes (fig. 8(a)) in the troposphere. On the other hand, the mean vertical motion of the troposphere is a very small quantity and usually an order of magnitude less than the other parameters used to ascertain it. Therefore, considering that several thermodynamic processes were assumed nearly zero for this study, a complete success in relating vertical motion and temperature should not be expected in the troposphere.

3. Conclusions

This study has demonstrated that based on constant pressure charts of 5-day intervals, large scale features of horizontal stratospheric heat transport in the eddy flow can be described with considerable detail. A study of waves 1 through 4 at this resolution appears adequate in that these waves carry most of the available potential energy in the stratosphere as it is converted from zonal to eddy flow, or vice versa. However, problems of vertical correspondence could not be completely resolved in a study of only three levels.

The construction of 500-mb heat transport charts possibly requires smaller intervals between days or some form of graphical smoothing should be performed. It appears that strong contributions from short waves with a duration of only a few days was the source of the problem.

An attempt was made to simplify the complexities of the 500-mb heat transport chart. It was found that by constructing this chart for only the long waves (1, 2 and 3) the pattern was slightly improved and afforded a better working tool. Possibly other combinations of waves would give still better results. However it was noted that within certain groupings of wave numbers, one wave will tend to contribute in an opposite sense from the other waves in the spectrum. This is possibly a manifestation of the Fourier method. For example, wave 3 appeared to assume the difference in variance that corresponded with changes in waves 1 and 2.

The findings from this spectral treatment of the heat transport in the atmosphere has defined how the stratosphere thermally responds to divergence of heat transport and vertical velocities. From the large scale phenomena studied the following results were found:

- 1.) The spectrum of heat transport was subject to major changes with respect to time and height. During 1959-60, wave number one dominated the stratospheric heat transport, however (Boville 1961) waves number one and two were both large contributors in the previous year. These spectral changes of transport varied slowly and systematically during the period studied.
- 2.) The correlation in the vertical of the maxima and minima heat transport centers was usually negative in mid-latitudes. At high latitudes the long waves were found strongly related vertically throughout the atmosphere, whereas in the low latitudes the shorter waves occasionally extended from the troposphere upward to the 25-mb level.
- 3.) Northward heat transport corresponded with changes in the mean temperature field and this correspondence was most evident at 25 mb.
- 4.) The expected stratospheric temperature changes stemming from the divergence of heat transport were either dampened or reversed by vertical motion.

- 5.) The air of the polar night low at 25 mb was generally ascending and occasionally attained a maximum velocity of about 1 cm per sec. The strongest subsidence at the 25-mb level occurred near latitude 55N and the maximum velocity was about 0.5 cm per sec.
- 6.) At high latitudes the stratospheric vertical motion patterns extended down to the 500-mb level.
- 7.) The heat transport and vertical motion patterns were usually of at least 10 to 15 days duration in the stratosphere and during strong warmings extended from low latitudes northward to the polar regions.

References

- Benton, G.S. and A.B. Kahn, 1958: 'Spectra of large-scale atmospheric flow at 300 millibars', J. Meteor., 15, 404-410.
- Boville, B.W. and M. Kwizak, 1959: 'Fourier analysis applied to hemispheric waves of the atmosphere', Meteorological Branch, Canada, TEC-292.
- Boville, B.W., 1960: 'The Aleutian stratospheric anticyclone', J. Meteor., 17, 329-336.
- Boville, B.W., 1961: A dynamical study of the 1958-59 stratospheric polar vortex, Publication in Meteorology No. 36, Arctic Meteorology Research Group, McGill University, Montreal, Canada, 134 pages.
- Craig, R.A. and W.S. Hering, 1959: 'The stratospheric warming of January-February, 1957', J. Meteor., 16, 91-107.
- Godson, W.L., 1959: 'The application of Fourier analysis to meteorological data', Meteorological Branch, Canada, TEC-295.
- Hill, C.E., 1963: A multi-level study of heat transport, Thesis, McGill University, Montreal, Canada, 72 pages.
- Lorenz, E.N., 1955: 'Available potential energy and the maintenance of the general circulation', Tellus, 7, 157-167
- Mintz, Y., 1955: 'Final computation of the mean geostrophic poleward flux of angular momentum and of sensible heat in the winter and summer of 1949', U.C.L.A.*

*'Investigations of the general circulation of the atmosphere',
Final Report of General Circulation Project No. AF19(122)-48, Dept. of
Meteor., University of California.

- Murakami, Takio, 1962: 'Stratospheric wind temperature and isobaric height conditions during the IGY period', M.I.T. Report No. 5, 213 pages.
- Murgatroyd, R.J. and R.M. Goody, 1958: 'Sources and sinks of radiative energy from 30 to 90 km', Quart. J.R. Met. Soc. 84, 225-234.
- Murgatroyd, R.J. and F. Singleton, 1961: 'Possible meridional circulation in the stratosphere and mesosphere', Quart. J.R. Met. Soc., 87, 125-135.
- Ohring, G., 1958: 'The radiation budget of the stratosphere', J. Meteor., 15, 440-451.
- Pisharoty, P., 1955: 'The kinetic energy of the atmosphere', U.C.L.A.*
- Tewele, S., 1963: 'Spectral aspects of the stratospheric circulation during the IGY', M.I.T. Report No. 8, 191 pages.
- Tewele, S. and F.G. Finger, 1960: 'Reduction of diurnal variation in the reported temperatures and heights of stratospheric constant pressure surface', J. Meteor., 17, 177-194.
- Van Mieghem, J., 1960: 'Zonal harmonic analysis of the northern hemisphere geostrophic wind field', Union Geodesique Et Geophysique Internationale, Monographie No. 8, Janvier 1961, I.A.M.A.P., Presidential Address, Helsinki, 27 July 1960.
- Van Mieghem, J., P. Defrise and J. Van Isacker, 1959: 'On the selective role of the motion systems in the atmospheric general circulation', The atmosphere and the sea in motion (B. Bolin ed.), New York, Rockefeller Inst. Press and Oxford Univ. Press, 230-239.

*'Investigations of the general circulation of the atmosphere', Final Report of General Circulation Project No. AF19(122)-48, Dept. of Metero., University of California.